



MARMARA UNIVERSITY
INSTITUTE FOR GRADUATE STUDIES
IN PURE AND APPLIED SCIENCES



**PREPARATION AND CHARACTERIZATION
OF BACTERIAL CELLULOSE AND
POLYETHYLENE OXIDE BLEND FILMS**

FATMANUR İLHAN

MASTER THESIS

Department of Chemical Engineering

Thesis Supervisor

Asst. Prof. Dr. MÜGE SENNAROĞLU BOSTAN

Thesis CO- Supervisor

Prof. Dr. MEHMET SAYIP EROĞLU

ISTANBUL, 2022



MARMARA UNIVERSITY
INSTITUTE FOR GRADUATE STUDIES
IN PURE AND APPLIED SCIENCES



**PREPARATION AND CHARACTERIZATION
OF BACTERIAL CELLULOSE AND
POLYETHYLENE OXIDE BLEND FILMS**

FATMANUR İLHAN

(524517001)

MASTER THESIS

Department of Chemical Engineering

Thesis Supervisor

Asst. Prof. Dr. MÜGE SENNAROĞLU BOSTAN

Thesis CO- Supervisor

Prof. Dr. MEHMET SAYIP EROĞLU

ISTANBUL, 2022

ACKNOWLEDGEMENT

First of all, I would like to express my deepest thanks to my advisor Asst. Prof. Dr. MÜge Sennarođlu Bostan for her guidance, endless support, patience, and motivation throughout my thesis. I would like to emphasize my sincere gratitude to my co-advisor Prof. Dr. Mehmet Sayıp Erođlu for help, immense knowledge, and valuable advice.

I sincerely thank Lect. Semra Ünal, Sümeyye Cesur, İdil Yemişer for their help. I would also like to present my thanks to Marmara University Scientific Research Project Coordination Unit (BAPKO) for the financial support. (Project Number: Fen-C-YLP-120619-5723)

In addition to my manager Onur Karadaş for his constant support in both my professional and personal life, I would like to thank my Gondol Plastik employers Ümit Akçebe and Mehmet Akçebe for giving me experience in the workforce while I was completing my master's degree.

And finally, I would like to thank my dear mother Zarife Sarigül, my dear father Turgut Sarigül, and my career mentor brother Ozan Sarigül, who have supported me throughout my life, and offer me endless love. I would also like to thank my husband, Alperen İlhan, for encouraging me and always being there for me.

July, 2022

Fatmanur İLHAN

TABLE OF CONTENTS

ACKNOWLEDGEMENT	i
TABLE OF CONTENTS	ii
ÖZET.....	v
ABSTRACT	vi
CLAIM FOR ORIGINALITY	vii
SYMBOLS	ix
ABBREVIATIONS.....	x
LIST OF FIGURES.....	xii
LIST OF TABLES	xiii
1 INTRODUCTION.....	1
1.1 Aim and Significance of the Study.....	1
1.2 Bacterial Cellulose.....	2
1.2.1 Production Methods of BC.....	4
1.2.1.1 Static Culture Method	5
1.2.1.2 Agitated/ Shaking Culture Method	5
1.2.1.3 Bioreactor Method	5
1.2.2 Applications of BC.....	6
1.2.2.1 Biomedical and pharmaceutical Industry.....	6
1.2.2.2 Cosmetic Industry	7
1.2.2.3 Food Industry	8
1.2.2.4 Paper Industry	9
1.2.2.5 Packaging Industry.....	10
1.2.2.6 Other Applications	11
1.3 Chitosan.....	11
1.4 (Poly) Ethylene Oxide	14

2	MATERIALS AND METHODS	16
2.1	Materials	16
2.2	Methods	16
2.2.1	Preparation of BC	16
2.2.2	Acid Hydrolysis of BC	16
2.2.3	Preparation of CH-PEO-BC films.....	17
2.3	Characterization of Blends	18
2.3.1	SEM & TEM	18
2.3.2	AFM	19
2.3.3	FT-IR.....	19
2.3.4	DSC	19
2.3.5	TGA.....	19
2.3.6	Stress-Strain Tests	20
2.3.7	DMA.....	20
3	RESULTS AND DISCUSSION	21
3.1	SEM & TEM	21
3.2	AFM.....	22
3.3	FT-IR	23
3.4	DSC	25
3.5	TGA	26
3.6	Stress Strain	29
3.7	DMA.....	30
4	CONCLUSIONS	34
	REFERENCES.....	35
	APPENDIXES	46
	Appendix A	46

Appendix B	48
AUTOBIOGRAPHY	49

ÖZET

BAKTERİYEL SELÜLOZ VE POLİETİLEN OKSİT KARIŞIM FİMLERİNİN HAZIRLANMASI VE KARAKTERİZASYONU

Bu çalışmada, çözelti döküm yöntemi ile 4 farklı bileşimde bakteriyel selüloz (BC) (*Gluconacetobacter xylinus*'un mikrobiyal fermentasyonu ile üretilmiş), polietilen oksit (PEO) ve kitosan (CH) karışım filmleri hazırlanmıştır. Karışımların hazırlanmasında sabit oranda CH-PEO (%85-%15) ve farklı miktarlarda BC (%0, %2, %4, %6) kullanılmıştır. Hazırlanan filmlerin detaylı termal, mekanik, spektroskopik, morfolojik ve yüzey karakterizasyonu çalışmaları yapılmıştır.

BC'un asit hidrolizi için sülfürik asit kullanılmış, taramalı ve geçirimli elektron mikroskopi (SEM&TEM) analizleri BC'un kristalin ve oldukça gözenekli bir yapıya sahip olduğunu ortaya çıkarmıştır. Atomik kuvvet mikroskopi (AFM) ile filmlerin yüzey pürüzlülüğü belirlenmiş ve, BC miktarı arttıkça karışımların yüzey pürüzlülüğünün de arttığı gözlenmiştir. Hazırlanan filmlerin mekanik mukavemeti, stres-gerinim testleri ile belirlenmiş olup, sonuçlar artan BC miktarının gerilme değerinde ve kopma uzamasında artışa neden olduğunu göstermiştir. Dinamik mekanik analiz (DMA) ile karışım filmlerin camsı geçiş sıcaklıkları (T_g) ve zincirlerin dolaşma yoğunluğu (N) değerleri hesaplanmıştır. Sonuçlar, BC oranı arttıkça karışımların hem T_g hem de N değerinin arttığını göstermektedir. Karışımların termal analizi için diferansiyel taramalı kalorimetri (DSC) ve termal gravimetrik analiz (TGA) teknikleri kullanılmıştır. BC ilavesi PEO'nun kristalinitesini bir ölçüde bastırarak ve karışım filmlerinin termal stabilitesini etkilemiştir. CH ve BC herhangi bir erime noktası göstermediğinden ve tüm karışımlarda CH- PEO oranı sabit olduğundan, PEO'nun erime noktasındaki düşüş BC ilavesinden kaynaklanmaktadır. BC partiküllerinin gözenekli yapısı sayesinde zincirler arasındaki etkileşimi artırarak PEO'nun morfolojik yapısını bozduğu düşünülmektedir. BC partiküllerinin PEO zincirleri arasına girerek PEO'nun C-O-C eter oksijeni ile hidrojen bağı yapması kristal yapıyı etkilemiştir. Bu sonuçlar literatür bilgileri ile de desteklenmektedir.

Bildiğimiz kadarıyla CH ve PEO'nun karışımları üzerine literatürde birçok çalışma olmasına rağmen, umut verici yeni bir aktif gıda ambalaj malzemesi olabilecek BC dolgulu PEO-CH karışımların karakterizasyonu hakkında bir rapor bulunmamaktadır.

ABSTRACT

PREPARATION AND CHARACTERIZATION OF BACTERIAL CELLULOSE AND POLYETHYLENE OXIDE BLEND FILMS

In this study, 4 different compositions of bacterial cellulose (BC) (produced by microbial fermentation of *Gluconacetobacter xylinus*), polyethylene oxide (PEO), and chitosan (CH) blend films were prepared by solution casting method. A fixed ratio of CH-PEO (%85-%15) and different amounts of BC (%0, %2, %4, %6) were used. The detailed thermal, mechanical, spectroscopic, morphological and surface characterizations of the blend films were performed.

Acid hydrolysis was applied for the hydrolysis of BC and, scanning and transmission electron microscope (SEM&TEM) analyses revealed that obtained BC has a highly porous structure. AFM determined the surface morphology of the blend films and the surface roughness of blends increased upon the increased amount of BC, which may be attributed to BC enrichment on the blend film surface. Stress-strain tests determined the mechanical properties of the blends, and an increased amount of BC resulted in a slight increase in the stress value and elongation at break.

Glass transition temperatures (T_g) and degree of entanglement density (N) of the blend films were calculated by dynamic mechanical analysis (DMA), and both were increased with the amount of BC. The increase in T_g values was due to the filler effect of BC, which was placed between PEO and CH chains, preventing segmental movements to some extent. Differential scanning calorimetry (DSC) and thermal gravimetric analysis (TGA) were used for the thermal analysis of the blend films. The BC addition suppressed the crystallinity of PEO, and the thermal stability of blends was slightly affected by BC. CH and BC do not display any melting points and the ratio of BC to PEO is fixed in all blends. The decrease in melting point of PEO in blend composition was due to the interaction between BC and PEO chains. It is notable that the BC hindered the PEO crystallinity to some extent. This result was confirmed by Fourier transform infrared spectroscopy (FT-IR) results.

Although many studies on CH and PEO blends has been found in the literature, to the best of our knowledge, there is no report on the detailed characterization of the BC filled PEO-CH blends which may be a novel promising active food packaging material.

CLAIM FOR ORIGINALITY

PREPARATION AND CHARACTERIZATION OF BACTERIAL CELLULOSE AND POLYETHYLENE OXIDE BLEND FILMS

CH, PEO, and linear bacterial polysaccharide cellulose (BC) are all versatile materials with exceptional qualities. Although there are numerous studies on the blends of BC, CH, and PEO with different polymers, to the best of our knowledge, there is no report on the characterization of a BC filled PEO-CH blends films in the literature, which may be a novelty and promising as active food packaging material.

BC has some superior properties such as purity, mouldability, crystallinity, porosity, tensile strength, biodegradability, etc. Apart from BC, CH and PEO also have a wide range of applications in several industries with superior properties.

Unlike previous studies, in this study, BC particles were added to the blend of PEO and CH and its effect on the thermal, mechanical, morphological and surface properties was investigated. A comprehensive characterization studies was performed to elucidate the intermolecular interaction between BC particles and PEO and CH polymers. For this purpose, FT-IR, DSC, TGA, DMA, SEM&TEM, and AFM techniques were used. The SEM and TEM results showed that the BC has a porous surface structure, which was confirmed by the AFM findings. BC's porous structure resulted in a relatively rough surface on the PEO-CH blend films. FT-IR analysis of the blend films indicated the hydrogen bonds between CH and PEO. It is notable that the addition of BC to the blend films resulted in an increased intermolecular interaction leading to a more amorphous morphological structure.

TGA was performed to determine the effect of BC on the thermal stability of the blend films; with the increase of BC in the blend formulation, PEO showed higher thermal stability and lower weight-loss rate.

Since CH and BC did not show any melting point and the ratio of BC to PEO was kept constant in all formulations, the melting peaks observed in the DSC thermograms were due to the PEO melting behaviour. The melting point of PEO in blend films decreased with increasing BC, which inhibited the PEO crystallinity to some extent.

The effect of BC on the mechanical properties of the blend films were investigated by performing their stress-strain tests. A slight increase in the elongation and strain values was observed with the increasing amount of BC in the formulations.

DMA analysis was used to investigate the interaction between blend components. The higher storage modulus indicates the higher interaction and entanglement between polymer chains. BC increased the interchain interactions in the PEO-CH structure, which increased the mechanical stability and regularity of the blend films. The results were further confirmed by calculating the degree of entanglements of the blend films. It is notable that the BC acts as a molecularly compatible polymeric filler between PEO-CH chains.



SYMBOLS

β	: Beta
ΔH	: Enthalpy
E'	: Storage Modulus
E''	: Loss Modulus
g	: Gram
Hz	: Hertz
J	: Joule
m²	: Meter square
mg	: Miligram
min	: Minute
mL	: Mililiter
μm	: Micrometer
mm	: Milimeter
mPa	: Megapascal
nm	: Nanometer
°C	: Celcius
rpm	: Revolutions per Minute
Tan δ	: Damping
T_g	: Glass Transition Temperature
T_m	: Melting Temperature

ABBREVIATIONS

AFM : Atomic Force Microscopy

ANT : Anthocyanin

BC : Bacterial Cellulose

BCNW : Bacterial Cellulose Nano Whistle

CH : Chitosan

DD : Deacetylation degree

DI : Deionized

DMA : Dynamic Mechanic Analysis

DSC : Differential Scanning Calorimetry

DTG : Differential Thermal Gravimetry

FDA : Food and Drug Administration

GRAS : Generally Recognized as Safe

MW : Molecular Weight

N : Degree of entanglement density

PCL : Polycaprolactone

PEG : Polyethylene Glycol

PEO : Polyethylene Oxide

PHB : Poly(3-hydroxybutyrate)

PLA : Polylactic Acid

PMMA : Polymethylmethacrylate

RMS :Root-Mean Square

SEM : Scanning Electron Microscopy

TEM : Transmission Electron Microscopy

TEMPO : 2,2,6,6-tetramethylpiperidin-1-oxyl radical

TG : Thermal Gravimetry

TGA : Thermogravimetric Analysis

THY : Thymol

TOBC : TEMPO Oxidation



LIST OF FIGURES

Figure 1.1. Molecular structure of BC [18].....	3
Figure 1.2. Molecular structure of chitin (a) and CH (b) [85].....	12
Figure 2.1. 1.0 gram of the dry BC (a) and small pieces of BC (b)	16
Figure 2.2. BC, CH and PEO blends	18
Figure 3.1. TEM image of 400 nm of BC	21
Figure 3.2. SEM image of 2 μm of BC	22
Figure 3.3. AFM topographic images and surface cross-section analysis of (A) blend 1 (1 $\mu\text{m}\times 1 \mu\text{m}$) (rms: 18.8 nm), (B) blend 2 (10 $\mu\text{m}\times 10 \mu\text{m}$) (rms: 21.7 nm), (C) blend 3 (10 $\mu\text{m}\times 10 \mu\text{m}$) (rms:24.8 nm) and (D) blend 4 (4 $\mu\text{m}\times 4 \mu\text{m}$) (rms: 26 nm)	23
Figure 3.4. FTIR spectra of blends and BC.....	24
Figure 3.5. DSC curves of blends.....	26
Figure 3.6. TG curves of CH and PEO.....	27
Figure 3.7. DTG curves of blends	28
Figure 3.8. TG curves of the blends	29
Figure 3.9. Tensile strength values of blends	30
Figure 3.10. E' curves of blends	31
Figure 3.11. E'' curves of blends	32
Figure 3.12. Tan δ curves of blends	32
Figure A.1. Weight loss of blend 1	46
Figure A.2. Weight loss of blend 2	46
Figure A.3. Weight loss of blend 3	47
Figure A.4. Weight loss of blend 4	47
Figure B.1. Weight loss of PEO	48
Figure B.2. Weight loss of CH	48

LIST OF TABLES

Table 2.1. Composition of Blends	18
Table 3.1. RMS values of the blends	22
Table 3.2. DSC data of the blends and pure PEO.....	26
Table 3.3. DTG peak temperature	28
Table 3.4. Mechanical properties	30
Table 3.5. T _g values of blends.....	33
Table 3.6. N values of blends	33

1 INTRODUCTION

1.1 Aim and Significance of the Study

Food packaging plays a vital role in the world by preserving food and reducing food waste along the distribution chain. Unfortunately, with increased package use comes increased trash accumulation. Food is often packaged with materials that are not biodegradable and have various aspects that make recycling them challenging. Biodegradable polymers derived from natural resources have the potential to be used as raw materials in the creation of innovative food packaging alternatives. BC has some superior properties such as purity, high water holding capacity, crystallinity, porosity, biodegradability, high mechanical and chemical strength. What's more, it is a transparent, non-toxic, non-allergenic natural and biocompatible product, which makes it an ideal candidate as a food packaging material.

CH is the most available polysaccharide after cellulose with many advantageous properties such as nontoxicity, semi-crystallinity, biodegradability, biocompatibility. Although CH has a significant capacity for film formation, films made from pure CH have a comparatively high tensile strength and poor flexibility.

PEO's water solubility, hydrophilicity, high viscosity, and biocompatibility make it low-toxic, semicrystalline, bioadhesive, and mucoadhesive polymer. On the other hand, its film forming capability is restricted when used alone. However, its flexibility and mechanical strength may improve when mixed with other biocompatible polymers, making it a favored component for blend formulations.

This thesis aimed to prepare biodegradable and biocompatible BC filled CH and PEO blend films to investigate their potential as a novel food packaging alternative material. Other primary goal was also their detailed characterization using thermal (DSC, TGA, DMA), spectroscopic (FT-IR), mechanical (stress-strain test), morfological (SEM, TEM), surface (AFM) techniques. The BC filled non-toxic biodegradable and biocompatible blend films might be a novel promising active food packaging material. Thus, the blend films with enhanced mechanical, and thermal properties specify the significance of this thesis.

1.2 Bacterial Cellulose

Cellulose was discovered by Payen in 1838. However, the first study on BC was published by Brown in 1886. He studied the use of glucose as a carbon source in manufacturing cellulose, which is generated by acetic acid bacteria [1, 2].

The most plentiful, affordable, and widely accessible linear polysaccharide in nature is cellulose, which may be obtained from plants or their wastes in the world. The fact that BC is made by bacteria rather than plants is the primary distinction between the two types of cellulose. Plant cellulose and BC have the same chemical content but different physical properties. Compared to cellulose derived from plants, BC has a structure that does not include pectin, lignin, or hemicellulose, which results in a higher level of chemical purity [3, 4]. Because it needs to be isolated from lignin and hemicellulose, obtaining cellulose from plants in its purest form is a challenging and expensive process [5]. In addition, the decline in the amount of land covered by forests has resulted in the search for alternate sources of cellulose. Research studies on BC have shown that although sharing the same chemical structure as cellulose from plants, BC is fundamentally different in its macromolecular structure and properties.

The degree of polymerization is generally between 2000-6000 [6], but in some cases, it reaches 16000 or 20000 [7]. On the other hand, this value varies from 13000 to 14000 on average in plants [8].

The surface area of BC is 200 times larger than plant cellulose [9, 10, 11]. Moreover, BC microfibrils are 100 times more refined and porous than plant cellulose [12, 13, 14, 15]. However, the fibril size, surface area, and porosity of BC are not always constant and may change over time depending on the production conditions, culture medium, and composition [13].

The bacteria that produce BC have different structures, morphologies, applications and properties compared to the production sources of cellulose. *Acetobacter xylinum*, also known as *Gluconobacter xylinum*, is the most abundant bacterial source, followed by *Acetobacter hansenii* and *Acetobacter pasteurianus*. It has also synthesised commonly available BC [16, 17].

It consists of a linear chain of several β -linked D-glucose units, as shown by the chemical formula $(C_6H_{10}O_5)_n$, where the number of units varies from hundreds to thousands depending

on the molecular weight of cellulose. Figure 1.1 shows the molecular formula of cellulose. Cellulose is most commonly used in producing paper and paper products [18].

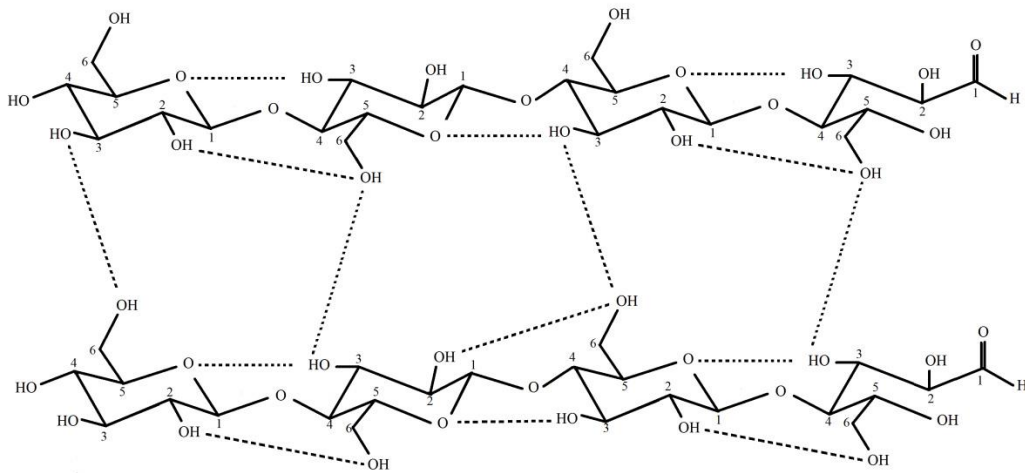


Figure 1.1. Molecular structure of BC [18]

In general, BC has some superior properties such as more purity, mouldability, crystallinity, hydrophobicity, porosity, tensile strength, biodegradability, water holding capacity, high thermal and chemical stability, mechanical strength, high degrees of polymerization, ultrafine nanoscale fibrous network and biological affinity compared to plant sourced cellulose [18, 19, 20, 21, 22, 23, 24]. Moreover, BC has a higher specific surface area ($37 \text{ m}^2/\text{g}$), higher aspect ratio and lower bulk density [16]. Especially purity, water holding capacity, biocompatibility [16], biodegradability [16] and nano-scale arrangement of BC make it a biocompatible material [25]. Moreover, BC is a transparent, non-toxic and non-allergenic natural product [4]. Depending on the production method, type of bacteria, and conditions of production, the size and shape of BC can be adjusted, giving it diverse application areas [12, 26].

In dried form, BC has extraordinary mechanical properties due to its crystalline nanofibrillar network [4]. Dry cellulose with a thickness of 0.01-0.5 mm can transmit sound waves quickly [9, 27, 28]. This feature allows the BC to be used as an acoustic membrane [27, 28, 29].

Several studies of BC and BC derivatives are being conducted to develop new films. Various polymers are blended with BC films to enhance or modify their properties and to increase the range of applications. There are two primary methods for obtaining BC with other polymers without compromising the film structure obtained during fermentation. One method is to include desirable agents in a fermentation medium. The BC films can also be deposited in the desired polymer solution bath. The most common application is as a reinforcing agent, using

nanocrystals or nano-whiskers of BC. Strong acids are typically used to hydrolyze BC films, breaking down the material's structure into nanofibers or nanocrystals [30]. The nanocrystals obtained have a high crystalline structure [22].

1.2.1 Production Methods of BC

BC's quality may change depending on the fermentation culture medium, microorganism, temperature, pH, growth circumstances (nutrition and oxygen), purification procedure, and drying methods [17, 23]. Classical cultural environment; it consists of a carbon and nitrogen source between pH 4-6 and other components necessary for bacterial growth. BC production efficiency increases when an abundant carbon source and a limited nitrogen source are available [31]. Because of the high cost of the carbon sources used in BC production, they are not used on a large scale [31, 32, 33]. Attempts have recently been made to lower production costs by employing industrial, forestry, and agricultural waste as carbon sources in BC production. Food processing wastes [34], beet and sugarcane molasses [35], various fruit wastes [33, 36], rice husk [37], wheat straw [38], cotton waste [39], coffee husk [40], olive milling residue [41], waste brewer's yeast [42], date syrup [43], and tree extracts [44] have been used in the production of BC in studies that are carried out so far [17].

The most popular application is utilizing nanofibers or nanowhiskers of BC as a reinforced material. BC is kept to hydrolysis using strong acids, splitting the structure into nanofibers or nanocrystals [45].

BC can be produced by several methods. Common production methods of BC are static culture method, agitated/ shaking culture method and bioreactor method. BC may show different physical, morphological and characteristics depending on the production method. The technique that is used to dry the BC affects its form, porosity, and mechanical characteristics [23]. The production conditions should be specified according to the desired product [17].

The most common techniques for separating the water are air drying at room temperature and oven drying. Freeze drying is another alternative in which water is frozen and then sublimed. Although the morphology and porosity of the fiber are preserved in this method, it deteriorates during drying at room temperature. Additionally, it was found that there was no appreciable difference in fiber diameter depending on the drying process and that BC films dried at ambient temperature had lower crystallinity than freeze-drying films [2, 23].

1.2.1.1 Static Culture Method

The most popular and conventional method is the static culture method which provides the perfect structure and properties. The gelatinous form of BC ends up at the surface of the nutrition medium [17].

The static culture method has a low production rate and high cost. Therefore, the traditional static culture method limits cost-effective production and industrialization. The need for cost and industrialization has led to the exploration of new production methods. So, production methods of less expensive wastes and different types of bacteria have been tried [2, 46].

Culture time, bacterial strains, and nutrition time affects the production of BC.

1.2.1.2 Agitated/ Shaking Culture Method

The slow and costly production rate of the static culture method created the shaking/shaking method.

There is a direct correlation between the amount of oxygen and the production of BC, but also excessive oxygen reduces production efficiency. Therefore, it is critical to optimize the amount of oxygen [17].

The products are obtained in the form of asterisk-like, sphere-like, pellet-like or irregular masses with the agitated/shaking culture method [17]. Rotational speed, bacterial strains, and culture time affects the production of BC.

Unfortunately, due to its low efficiency and high cost of production, this culture method is unsuitable for utility or industrial scale production. When the static culture method and the agitated culture method were compared, it was discovered that the production of BC was not greatly increased by the agitated culture method [46]. The crystallization coefficient and crystal size of cellulose obtained by agitated culture are smaller than that obtained by static culture [47].

1.2.1.3 Bioreactor Method

As previously described, the agitated culture method did not significantly increase the production of BC. The use of bioreactors has emerged as a result of new searches for high productivity, low cost and industrial scale production [46].

Numerous efforts have been undertaken in this direction, and several reactors that have been created to boost BC synthesis productivity are being examined. Enriched oxygen bioreactors, rotating disc bioreactors, modified static bioreactors, etc. have been reported to produce more efficient BC. Rotational speed, bacterial strains and culture time affected the production of BC according to investigations of the bioreactor method [2, 46].

1.2.2 Applications of BC

There are numerous ways to apply and use BC and BC derivatives in diverse regions such as food industry, cosmetics, waste purification, parchment, optoelectronic, bioelectronics, biosensors, security paper, electric instrument, batteries, e-paper and e-book tablets etc. [26, 48].

BC can be in various shapes such as slice, powder, slurry, beads, pieces, sponges, cubes and film for different purposes [12].

1.2.2.1 Biomedical and pharmaceutical Industry

The water holding capacity and the water release rate are one of the most important properties for biomedical applications [13].

BC and BC-based composites can be used for dental grafting, artificial cornea, artificial skin, wound dressing, drug delivery system, bone tissue engineering, meniscus implants, contact lenses, bioanalysis, hemodialysis, enantio-separation, medical pads, artificial blood vessels, antimicrobial activities, diagnostic sensors, biosensors, dura mater replacement and hemostatic materials [2, 13, 26].

In burn treatment, it has been reported that it has a healing effect on the burned areas [49, 50, 51], due to BC's sterilizable, tissue-compatible, porous, elastic, tangible, and water-adsorbing properties; wounds heal faster, infection formation is prevented in injured areas, pain is reduced by adsorbing the heat of the burned area in burn cases, and the spread of the wound in the tissue is prevented [51]. Instead of animal-derived collagen coaters, BC-containing coaters [Rensselaer Polytechnic Institute, USA] are used as wound sealants in the treatment of ulcers. It is stated that BC produced from *K. xylinum* has a wound-healing effect [51], and BC fibers can be used as artificial blood vessels [49, 52, 53].

Because BC is not biodegradable in the human body and shows low bioactivity property, its applications in tissue engineering are restricted [54].

Alginate/ BC nanocrystals, collagen composite hydrogel [55], and gelatin and BC composite sponges [54] were investigated for tissue engineering in separate studies. These investigations were studied for tissue engineering, and according to these studies, results show that it may have great potential as a scaffold for tissue engineering [54].

BC modified with CH was studied to investigate the biocompatibility of surgical meshes. Unfortunately, the tested material did not cause any allergic reactions or pathological changes in organs. So the results proved that this material could be integrated with tissues and suitable for the human organism [56].

BC mixed with collagen was reported to improve the thermal and mechanical properties. According to the report, BC/collagen composite films exhibited improved tensile strength and elongation. These results are essential for the use in wound dressings, artificial skin development, and optimization [57].

The created 3D composite scales have the potential to improve significantly bone implants for biomedical purposes. They are made of a composite of BC with polycaprolactone, gelatin, and hydroxyapatite [58].

Investigations were conducted to determine how the addition of BC nano whiskers (BCNW) affects the porous structure, mechanical characteristics, hydrophilicity, and water absorption behavior of poly(lactic) acid (PLA). It has been discovered that adding BCNW to PLA enhances its pore structure and increases its porosity, significantly raising its tensile strength, modulus, and compressive strength as well as its surface hydrophilicity and water holding capacity. The findings of this work demonstrated the potential of the BCNW/PLA composite for tissue engineering and medication delivery [59].

Extremely strong carboxymethyl cellulose/PEO mats and electrospun mats were developed with the included plant extracts, and studies were conducted on their suitability in the field of wound dressing applications. The results are encouraging for possible clinical use in treating acute wounds, where plant extracts might help wounds heal more quickly due to their antibacterial and antioxidant properties [60].

1.2.2.2 Cosmetic Industry

BC can be used to make facial masks, scrubs, and personal cleaning formulations, as well as fingernail polish and artificial nails. It can also be used in moisturizing creams due to its high degree of hydration and skin penetration [12, 61].

Using BC as a mask and its properties was investigated by performing sensory analysis. The results indicated that the formulations released from the mask to the skin could be applied cosmetically [62].

Other applications of BC are nail polish and artificial nails. The rheological properties of BC provide stability to suspensions [61]. BC is used in the cosmetic industry to increase the absorption of creams, tonics, and nail polishes [27, 50].

Composite gels of BC and polyethylene glycol diacrylate are characterized structurally and mechanically. This study has demonstrated that gels' viscoelastic behavior has enormous potential in the medical and cosmetic industries [63].

1.2.2.3 Food Industry

It is applicable in the food sector for traditional desserts, thickening, stabilizing, gelling, and suspending agents, low cholesterol food additives, vegetarian food, food ingredient and dietary aid, enzyme immobilization, and food packaging materials [12, 64, 65].

Since BC is a dietary fiber, it was classified as 'Generally recognized as safe' (GRAS) by the US Food and Drug Administration (FDA) in 1992.

Traditional dessert

BC is frequently used as a raw material for Nata de Coco, a typical sweet confection from the Philippines that is popular across Southeast Asia [12, 61, 64]. Its use started by adding to diet drinks in BC Japan in 1992. A tea-based beverage called Kombucha or Manchurian tea is fermented tea. Cellulose results from this process following fermentation [61, 65, 66].

Low cholesterol food ingredient and food additive & dietary aid

Because of its high water holding capacity and ion exchange capacities, BC can be used as a laxative and low cholesterol diet material. Another application of the BC is monascus extract, which is obtained from natural red-pigmented mould in combination with BC as vegetarian meat [12, 66, 67].

It is stated that low-calorie food products can be produced with BC. For example, the addition of 10% BC to meatballs is accepted as a potential product that can be added to meatballs as a substitute for fat in emulsified meat products, showing similar properties to control samples in sensory and shelf life of meatballs; these meatballs are juicy and chewy [68]. It has been

stated that surimi products, in which BC is used instead of oil, have a superior water holding capacity, preserve the unique structure of the product, and have better mechanical properties [69]. In a study on how BC is used to make foods like mayonnaise, sausage, and white cheese [70] it was stated that mayonnaise with 20% reduced fat and 1% BC added was the most preferred product with the highest stability as a result of sensory evaluation. In the study, it was also stated that adding BC instead of fat in sausage production carries the usual sausage characteristics, the calorie decreases, and the dietary fiber content increases, and the melting does not occur in white cheese with BC addition.

Gelling agent

To ensure better texture and firmness, the gel strength of Tofu made by coagulating and pressing soy milk can be significantly increased by adding % 2- % 3 BC [12, 64].

Suspending agent

BC added to chocolate drink which is produced by the agitated culture method, prevents precipitation of the cocoa because of keeping the cocoa particles by the BC [64].

Stabilizing agent

It has been stated that the product containing BC maintains its moisture content for at least one month of storage. The BC-containing ice cream kept its shape for at least 60 minutes after being taken out of the freezer, whereas the BC-free ice cream melted completely at the same time [64, 71, 72].

1.2.2.4 Paper Industry

The main usage area of BC is paper production. BC increases the gloss and reduces the weight of papers and paper based cardboards. On the other hand, BC can be used to produce electronic papers apart from the traditional paper production processes. Also, the paper produced from the BC is entirely pure, and has higher dimensional stability and water retention compared to synthetic paper [61].

The use of BC in manufacturing premium paper has been suggested due to its superior mechanical qualities. According to the manufacturer, these papers with BC absorb fillers and colors well, are elastic and permeable, have a high water holding capacity, and are resistant to tearing and burning [49, 73].

It has been reported that handmade papers and documents that are used in the modification of historical documents and that have a small amount of BC added to their fibrils have increased resistance to abrasion [49, 74], papers containing 3% BC have similar surface properties as 20% coated rotogravure paper, papers with 1% BC content are included in the ISO 9706:1994 standard [49, 75].

1.2.2.5 Packaging Industry

The reason for investigating food packaging alternatives is to preserve food and minimize food waste throughout the distribution chain. Excessive packaging consumption, however, results in excessive waste production. High, low, and very low-density polyethylene, polyethylene terephthalate, polyvinyl chloride, polystyrene, and polypropylene are the most common materials used in food packaging. However, they do not biodegrade and are extremely difficult to recycle. The creation of innovative food packaging materials may use biodegradable polymers obtained from natural sources. The use of BC in the food industry is of great interest due to its excellent and unique features compared to other polysaccharide-based polymers. Many studies have been conducted on the use of using BC-reinforced structures as packaging materials.

A smart packaging study was carried out by including anthocyanin obtained from purple potatoes in TEMPO (2,2,6,6-tetramethylpiperidin-1-oxyl radical) oxidation (TOBC) of BC. Thymol (THY), a phenolic monoterpene derived from thyme with antibacterial activity, has been added to monitor food quality in real time and extend the durability of food products and produce smart packaging. THY is classified as GRAS by the FDA and is allowed to be widely used as a food additive and preservative. However, like THY in BC, it has been classified as GRAS by FDA. A study was conducted to develop a new smart and active food packaging film by adding THY and anthocyanin-rich purple potato extract (ANT) to TOBC films. Unlike other studies, freshness and real-time detection of food quality are carried out in this study. The microstructure, mechanical properties, and ultraviolet (UV) protection behavior of the prepared films were investigated, as well as their colorimetric response to ammonia, antioxidant, antibacterial, and reuse performances, and real-time monitoring and preservation of shrimp freshness. According to the study, TOBC/THY/ANT film is a promising and environmentally friendly food packaging material [76].

The morphological, optical, barrier, and tensile properties of thermoplastic corn starch nanobiocomposites containing BCNW were investigated and characterized. Morphological studies showed an improvement in the barrier properties of BCNW, hardening in the material structure, and a decrease in the elongation at break. In the second part of this study, electrospun poly(3-hydroxybutyrate) (PHB) fibers of nanobiocomposite films were homogenized and coated to keep moisture out of the nanobiocomposite. The barrier properties of the multilayer structures created in this manner were significantly enhanced [77].

Biodegradable composite films of BC, curcumin and CH were studied. The study's findings led to the conclusion that the films produced had strong mechanical characteristics and antioxidant properties and might provide effective active packaging for meat and other high-fat meals [78].

1.2.2.6 Other Applications

BC can also be used in the electronic industry. BC reinforced polyurethane-based resin nanocomposites were studied to investigate the effects of physical, mechanical and dielectric properties. This study shows that BC can be used for an electronic display device in the future [79].

BC has a good mesh structure and suitable material, is biodegradable and has high water resistance, and is a suitable material for food packaging [12, 45]; however, it has been stated that it does not have antioxidant and antibacterial properties to prevent food contamination. Therefore, much more effective results are obtained due to the use of BC with antimicrobial and antioxidant substances [80]. It has been stated that the esterified BC membrane has better barrier properties against vapor and gas than the original BC membrane as a packaging material [81]. Although polylactic acid (PLA) is a thermoplastic polyester that is biodegradable and renewable, it is not appropriate for specific applications; the combination of BC and PLA has been found to be both transparent and have better mechanical properties [82].

1.3 Chitosan

CH is a linear amino polysaccharide derived from chitin deacetylation. Chitin, on the other hand, is a natural biopolymer found in shellfish shells and is the second most abundant on the planet after cellulose. CH is a naturally occurring polymer that has been approved by FDA. It

is composed of N-acetyl-D-glucosamine and a randomly oriented β -(1-4)-linked D-glucosamine (deacetylated unit) (acetylated unit). It is a nontoxic, semi-crystalline [83, 84], biodegradable, biocompatible linear polysaccharide. It has a similar structure to cellulose and is generally compatible with dietary applications [84].

It is shown with the chemical formula of $(C_6H_{11}NO_4)_n$. The molecular structures of chitin and CH are shown in Figure 1.2 [85].

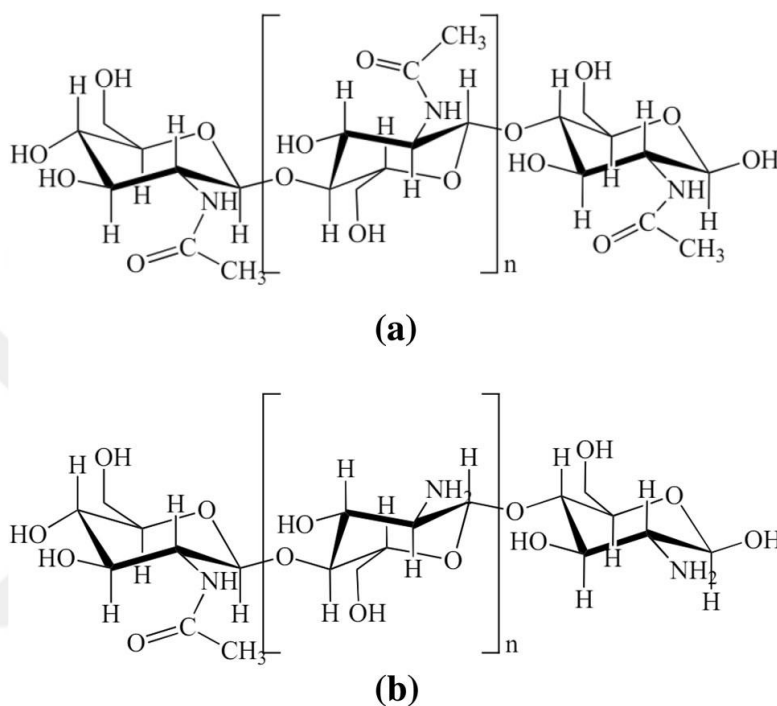


Figure 1.2. Molecular structure of chitin (a) and CH (b) [85]

Chitin; a white, hard, inelastic, and nitrogenous compound is the second most abundant and available polysaccharide after cellulose. Crustaceans and insects' exoskeleton is mainly composed of chitin [86]. On the other hand, chitin is present in marine invertebrates, fungi, and yeasts. About 70% of the amount of chitin in nature which is more than 1000 tons per year, comes from marine species. It can be produced from the fishery industry as a by product, so chitin can be considered as a regenerating raw material [85, 87]. CH is a biocompatible polymer used for dietary use in Japan, Italy, and Finland. In 2005, the FDA recognized it as GRAS [87].

CH is more active than chitin, as evidenced by the hydroxyl groups on every repeating unit and the amine groups on each deacetylated unit. Therefore, CH is more accessible to chemical modification to change its mechanical and physical properties. CH's structure is of great significance since its physicochemical characteristics are influenced by its deacetylation and

low crystalline regions. These characteristics are affected by the degree of deacetylation (DD), crystallinity, molecular weight (MW) and degradation methods [84].

CH can be used in the pharmaceutical and medical industry, paper production, textile wastewater treatment, biomedical, chemical [45], cosmetics, food, and agriculture industries. Thanks to superior properties such as biocompatibility, biodegradability, proliferation [88], good cell adhesion [88], anti-tumour, analgesic, anti-inflammatory [84], nontoxicity and antimicrobial activity of CH, it can be taken into consideration in the biomedical application such as tissue engineering, artificial kidney membrane, wound healing /wound dressing, artificial skin, bone damage, articular cartilage, liver, nerve, artificial tendon, burn treatment, blood anticoagulation, blood vessel, application for hernia, absorbable sutures, antimicrobial applications, drug delivery systems, cancer treatment, catheter, ophthalmology [83, 85, 87, 89]. Solubility and antimicrobial activity are two more characteristics that make it an ideal polymer to combine with BC [45].

Furthermore, CH increases the adhesion due to its mucoadhesive property and so the contact time of drug penetration is increased. On the other hand antimicrobial activity restricts the ability of infection [83].

Despite all these advantages, CH also has some disadvantages such as poor solubility, poor mechanical properties [88] and a high degradation rate [88, 90]. Poor solubility problem affects the use of pharmaceutical formulations. It can be soluble in acidic solution which is under the pH of 6.5. The using area and chemical modification of CH is restricted because of the solubility problem [83].

Another restriction effect of its use in the biomedical industry is that the CH film is very rigid and brittle. So some modifications can be made to improve the flexibility [91].

Films made from CH, derivatives, and its mixture are widely available in the literature. For example, CH and poly vinyl alcohol films were investigated for the treatment of skin lesions [90].

Polyethylene glycol (PEG) crosslinked CH was investigated to improve the mechanical properties [91]. In this investigation, diepoxy PEGs crosslinked CH films were compared with CH/PEG blend films. Thermal stabilities and elongation yield were found to be high in this study.

Re-acetylated CH and anti-aging compounds films were studied to research their use as a cosmetic mask [92]. CH was re-acetylated and produced more flexible and less durable films. Moreover, it allowed the anti-aging compounds to be released more into the skin. This behaviour supports its use as a cosmetic mask [92].

In collaboration with CH and polyvinyl alcohol, BC films were characterized according to mechanical and barrier properties. In this investigation, the results showed that BC films combined with CH and polyvinyl alcohol improved the mechanical, vapor permeability, thermal and optical properties, and can be used as a biopolymer for food packaging [30].

Studies have been done on CH/PEO nanofibers. The characterized nanofibers showed biodegradability and reduced cytotoxicity degree. The study concluded that CH/PEO nanofibers are suitable for wound healing applications [93].

In another study, the production of CH and PEO electrospun structure by spirograph-based mechanical system was carried out. Compatibility for wound dressing application with the additive of aloe vera into the prepared electrospun mat was studied, as promising materials [94].

1.4 (Poly) Ethylene Oxide

Although the three names are chemically equivalent, PEG has historically been used to refer to oligomers and polymers with molecular masses less than (20,000 g/mol), PEO to polymers with molecular masses greater than (20,000 g/mol), and POE to polymers of any molecular mass [95, 96]. While different molecular weights of PEG and PEO are used in different applications, different functionalities [96], have different physical properties due to chain length effects, and their chemical properties are nearly identical [95].

PEO, with a molecular formula of $(\text{CH}_2\text{CH}_2\text{O})_n$, has some recognizable properties such as biocompatibility, water solubility and ability of hydrogen bonding with water [97].

PEO is a biocompatible, linear polymer that has semi-crystalline structure with high gelation ability. PEO has some good properties such as excellent water solubility [96], hydrophilicity, non-toxicity [96], high chemical and thermal stability, and the possibility to increase recognition by the human immune system [96, 98, 99, 100, 101]. PEO is one of many materials for scaffolding that contains natural polymers such as collagen, CH, keratin, gelatin or polymethylmethacrylate (PMMA), Polyurethane, Polyethylene terephthalate, PLA, Polycaprolactone (PCL) synthetic polymer [94].

However, it is a rigid and crystalline polymer with some limitations in using film material alone. PEO is a nonionic polymer, and the ionic conductivity of PEO is limited because of the high degree of crystallinity [102]. Given its advantageous properties, it is possible to improve flexibility and mechanical strength by blending it with some natural biocompatible polymers.



2 MATERIALS AND METHODS

2.1 Materials

BC was generously supplied by the Technology Faculty of Marmara University and produced by microbial fermentation of *Gluconacetobacter xylinus*. PEO (300,000), Sulphuric acid (CAS#7664-93-9, 98% purity), and CH (1.86×10^5 g/mol) was supplied from Sigma–Aldrich and used as received.

2.2 Methods

2.2.1 Preparation of BC

Hestrin and Schramm medium, which contains D-glucose, peptone, yeast extract, disodium hydrogen phosphate, and citric acid, is used as the bacteria culture medium. The BC membranes are purified after being incubated in a stationary incubator, and they are then repeatedly submerged in deionized water (DI). The samples are dried in an oven after being sterilized by autoclave [103].

2.2.2 Acid Hydrolysis of BC

1.0 gr of BC was cut into small pieces to increase the surface contact area with sulphuric acid, thus leading to higher acid hydrolysis efficiency. The BC in the film form and the image after cutting into pieces is given in Figure 2.1. (Fig.2.1).



a)



b)

Figure 2.1. 1.0 gram of the dry BC (a) and small pieces of BC (b)

A solution containing 100 mL of 50 % sulfuric acid was prepared using sulfuric acid (98% purity) and mixed with 1.0 g of BC under magnetic stirring at 500 rpm. The mixture temperature was fixed at 45 °C to prevent overheating and further decomposition of the cellulose and carried out for 75 minutes. The hydrolysis reaction was ended by adding 10-fold cold DI water. The diluted suspension was then centrifuged with repeated washing with deionized water at 25 °C, 5000 rpm for 5 minutes until the pH value of 4 was reached. Further neutralization was carried out by the dialysis method for 10 days until neutrality. The final concentration of the suspension was calculated as ~0.82% w/v from the TGA method, and blend compositions were prepared from suspended BC based on this concentration without any drying process.

2.2.3 Preparation of CH-PEO-BC films

Four different compositions of films with 75-micron thickness were prepared based on increasing amounts of BC. In all compositions, the total amount of BC, PEO, and CH was fixed to be 0.75 grams for setting desired film thickness. The first film (blend-1) does not contain cellulose, while the fourth film is the most BC containing one. In all film compositions, the ratio of CH to PEO (M.W. 300.000) was fixed as 85:15 (w:w) based on a previous study [104]. The BC percentage weights were 2%, 4%, and 6%, while the CH/PEO ratio was kept constant. The percent compositions of blends are given in Table 2.1.

The blends were prepared separately by dissolving CH and PEO in 1% (w:w) acetic acid solutions for three days and degassing through a rotary evaporator for 45 minutes. CH has a molecular weight of 1.86×10^5 g/mol, as it was determined in previously study [104]. The degassed solutions were mixed at the desired ratios and were further stirred and degassed for 45 minutes. After that, the obtained clear polymer solutions were poured into Petri dishes. The blend solutions were allowed to dry with the caps half closed for about 1 month at room temperature and kept under 1 bar pressure, at 35 °C for 1 week to remove any traces of water and acetic acid. The completely dried films were easily removed from the Petri dishes, and their photographs are given in Figure 2.2.

Table 2.1.Composition of Blends

Sample code	Amount of PEO (%)	Amount of CH (%)	Amount of BC (%)
Blend 1	15.00	85.00	-
Blend 2	14.70	83.30	2
Blend 3	14.40	81.60	4
Blend 4	14.14	79.87	6

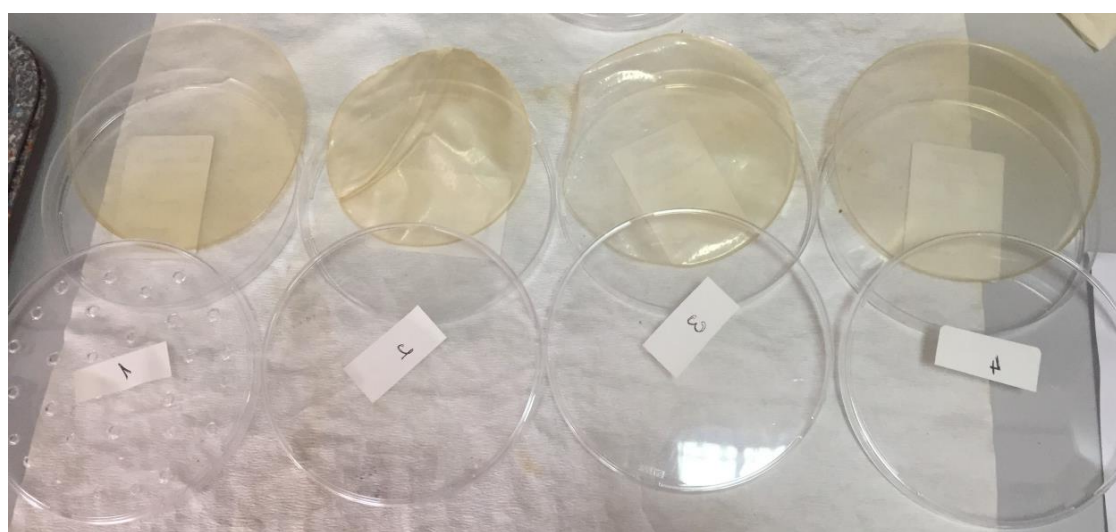


Figure 2.2. BC, CH and PEO blends

2.3 Characterization of Blends

SEM and TEM of BC after acid hydrolysis, AFM for surface morphology, FT-IR for determine the morphological structure, DSC and TGA for investigate the effects of hydrogen bonding on the morphology and thermal stability, stress-strain tests and DMA for mechanical properties of blends were employed.

2.3.1 SEM & TEM

Images of hydrolyzed BC were obtained using a HITACHI 5000 VP-FEG-SEM&EDS equipped with a Schottky Gun and a DEBEN-TEM detector. A drop of aqueous dispersion was applied to a conductive carbon ribbon and left at room temperature for 30 minutes before the images were taken.

SEM images were taken at 300 and 180,000 magnifications, whereas TEM images were taken at 15,000 and 100,000 magnifications in high vacuum mode with an acceleration voltage of 5 kV.

2.3.2 AFM

Microscopic techniques are typically used to explore the topography, roughness, and comparable morphological characteristics of surfaces. These qualities are essential for creating novel materials in materials science, biotechnology, and numerous other disciplines where the surface of the substrate is essential for the adhesion of other materials [105].

AFM (Hitachi Hitachi AFM5100N type instrument) was used to evaluate the blends' surface topography and phase separation morphology. The probe was triangular SI-DF-3P2 cantilever with a spring constant of 2.4 N/m, which was applied under contact mode. AFM images were recorded under ambient temperature and humidity by scanning 1.0x1.0 μm^2 area.

2.3.3 FT-IR

FTIR spectrometer was used to perform chemical analyses on blends (model 4700 Jasco, Japan). Automatic gain signals from 200 scans with a resolution of 1 cm^{-1} recorded a spectral range of 450-4000 cm^{-1} .

2.3.4 DSC

Among all thermal analysis methods, DSC is one of the most frequently utilized one. It is carried out by heating or cooling the sample with an inert reference to get information on thermal changes [106]. The compatibility and thermal stability of blends and the determination of melting and crystallization temperatures were evaluated using a Perkin Elmer Jade DSC and the data were evaluated using Pyris Software.

Measurements were performed under dynamic argon atmosphere with a flow rate of 200 $\text{ml}\cdot\text{min}^{-1}$ and a heating rate of 10 $^{\circ}\text{C}\cdot\text{min}^{-1}$ between -50 $^{\circ}\text{C}$ and 150 $^{\circ}\text{C}$.

2.3.5 TGA

TGA analysis of the blend films (7.0 mg) was performed using a Seiko-EXSTAR-TG/DTA7300 model thermogravimetry, and the data were evaluated by MUSE software. TGA measurements were carried out under the dynamic argon atmosphere (200 $\text{ml}\cdot\text{min}^{-1}$) at a heating rate of 10 $^{\circ}\text{C}\cdot\text{min}^{-1}$.

2.3.6 Stress-Strain Tests

Stress-strain tests were taken in tensile mode at 20 °C with a rate of 5 mm.min⁻¹ using an Instron 4411 tensile test machine. The results were analysed using Bluehill 2 software. The final tensile stress and strain values at the break of the blends were calculated and expressed as MPa and percent elongation, respectively.

2.3.7 DMA

DMA measures the mechanical properties of a sample as a function of temperature and provides information about the phase behavior, morphology and T_g temperatures of polymeric materials. Storage modulus (E') gives information about the stiffness of a material. The elastic behavior of a material is represented by the E' , which is in phase with the applied stress, while the viscous flow behavior of the material is represented by the loss modulus (E''). The mechanical damping factor ($\tan \delta$), the amount of the deformation energy released during each heat cycle, is obtained from the ratio of the E'' to the E' ($(E'')/ (E')$). A comparable oscillating strain results from applying a sinusoidal oscillating strain to the sample. Unless the material is entirely elastic, a phase difference (δ) occurs between the measured strain and the applied stress. The T_g value is obtained from the maximum peak position of the $\tan \delta$ curve recorded as a function of temperature [107]. The most typical DMA studies involve measuring the mechanical $\tan \delta$ and E' versus temperature at a single oscillation frequency [106,108]. The compatible blends display a greater degree of entanglement density compared to the incompatible blends. The degree of entanglement density provides information about the compatibility of blends and intermolecular interactions between polymer chains. The E' data could be used to determine N value using the equation (1), where E' is the storage modulus, R is the universal gas constant and T is the absolute temperature.

$$N = \frac{E'}{6RT} \quad \text{(Equation 1) [108]}$$

A Diamond model DMA analyzer produced by Shimadzu was used for the measurements. The data were evaluated by using the TA Universal Analysis software, and the sinusoidal oscillating standard tensile deformation mode was applied to the rectangular (10 mm x 10 mm x 0.07 mm) test specimens under a nitrogen atmosphere. The simultaneous measurement of E' , E'' , and $\tan \delta$ as a function of temperature was performed in multi-frequency mode (1, 2, 5,

10, 20 Hz). Data were collected between $-100\text{ }^{\circ}\text{C}$ - $+80\text{ }^{\circ}\text{C}$ temperature ranges at a heating rate of $2\text{ }^{\circ}\text{C}\cdot\text{min}^{-1}$.

3 RESULTS AND DISCUSSION

3.1 SEM & TEM

SEM and TEM images of the BC after acid hydrolysis were taken to determine the morphological structure of BC.

400 nm TEM analysis (Figure 3.1) and $2\text{ }\mu\text{m}$ SEM analysis (Figure 3.2) images show that the BC has a porous structure. This result is consistent with the fact that the E' is increasing, arising from the enhanced intermolecular interaction between the PEO and CH structures due to the porous structure of BC.

Similar results were also found in the literature which demonstrated that BC has a porous structure. Cazón and his friends agreed to porous structure with SEM images of BC in their blends composed of CH/polyvinyl alcohol and BC [45].

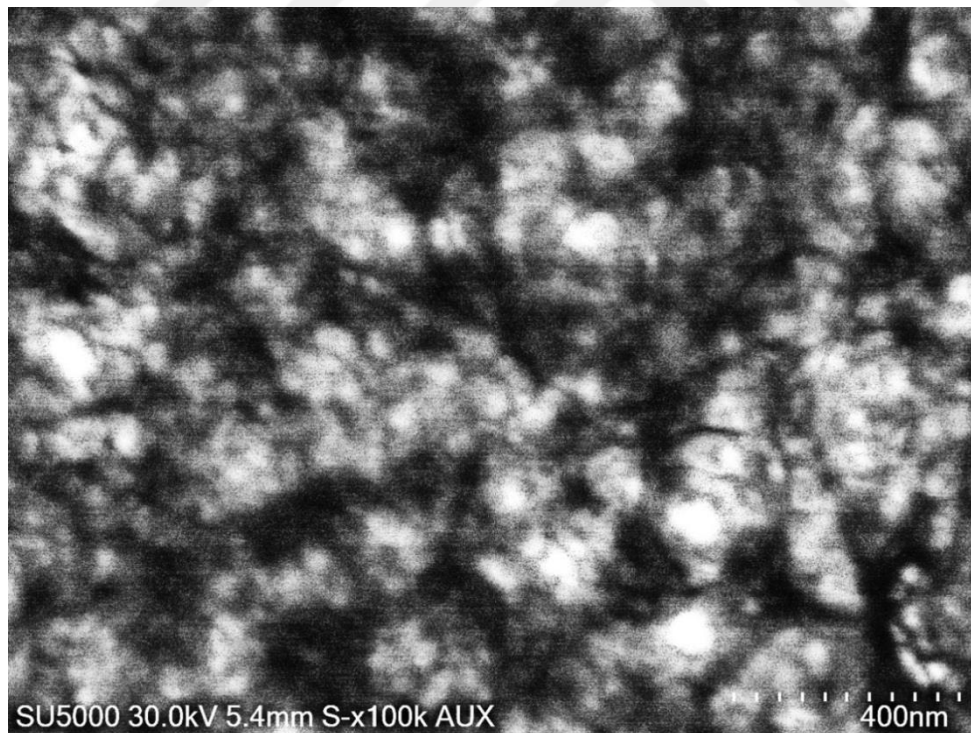


Figure 3.1. TEM image of 400 nm of BC

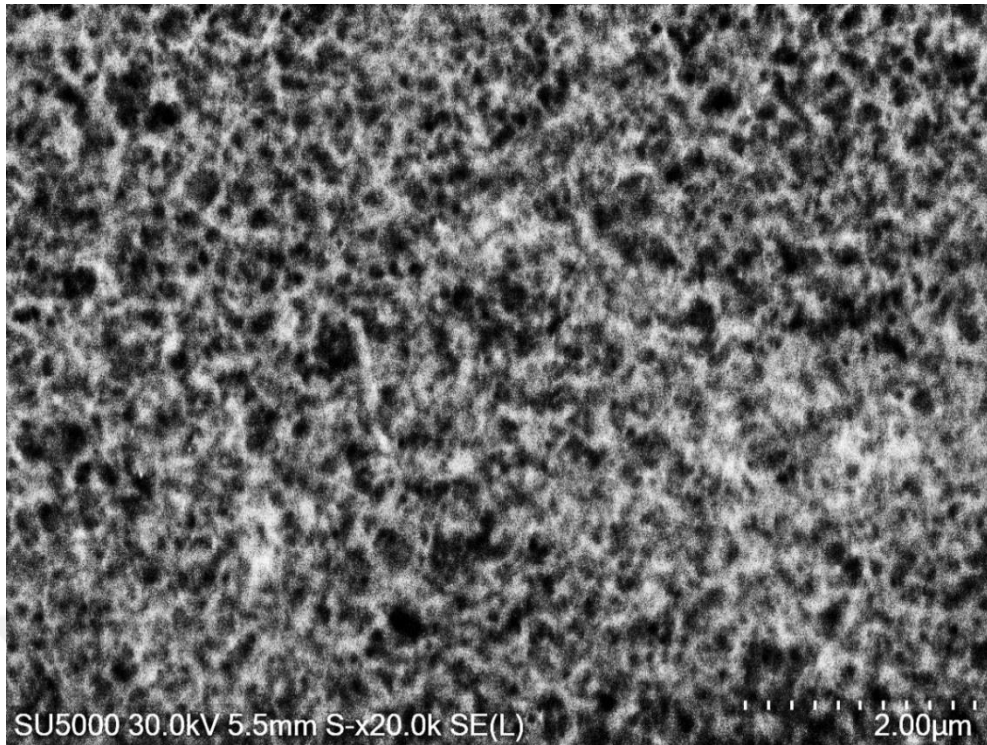


Figure 3.2. SEM image of 2 μm of BC

3.2 AFM

The AFM phase images and surface cross-section analysis of the blends was performed to evaluate the effect of BC on the surface topography of the blend films using tapping mode. The AFM images are shown in Figure 3.3. The root mean square roughness (RMS) of the blend films was increased from 18.8 nm to 26 nm as the amount of BC increased in the blend compositions, which may be attributed to BC enrichment on the blend surfaces [109]. These results agree with SEM & TEM results which revealed that BC surface is quite porous. The AFM measurements also indicate an interesting pattern concerning blends' surface morphology: the blends' opacity increases with a higher ratio of BC in the blend.

Table 3.1. RMS values of the blends

Sample code	Sq/RMS (nm)
	1CH
Blend 1	18.8
Blend 2	21.7
Blend 3	24.8
Blend 4	26

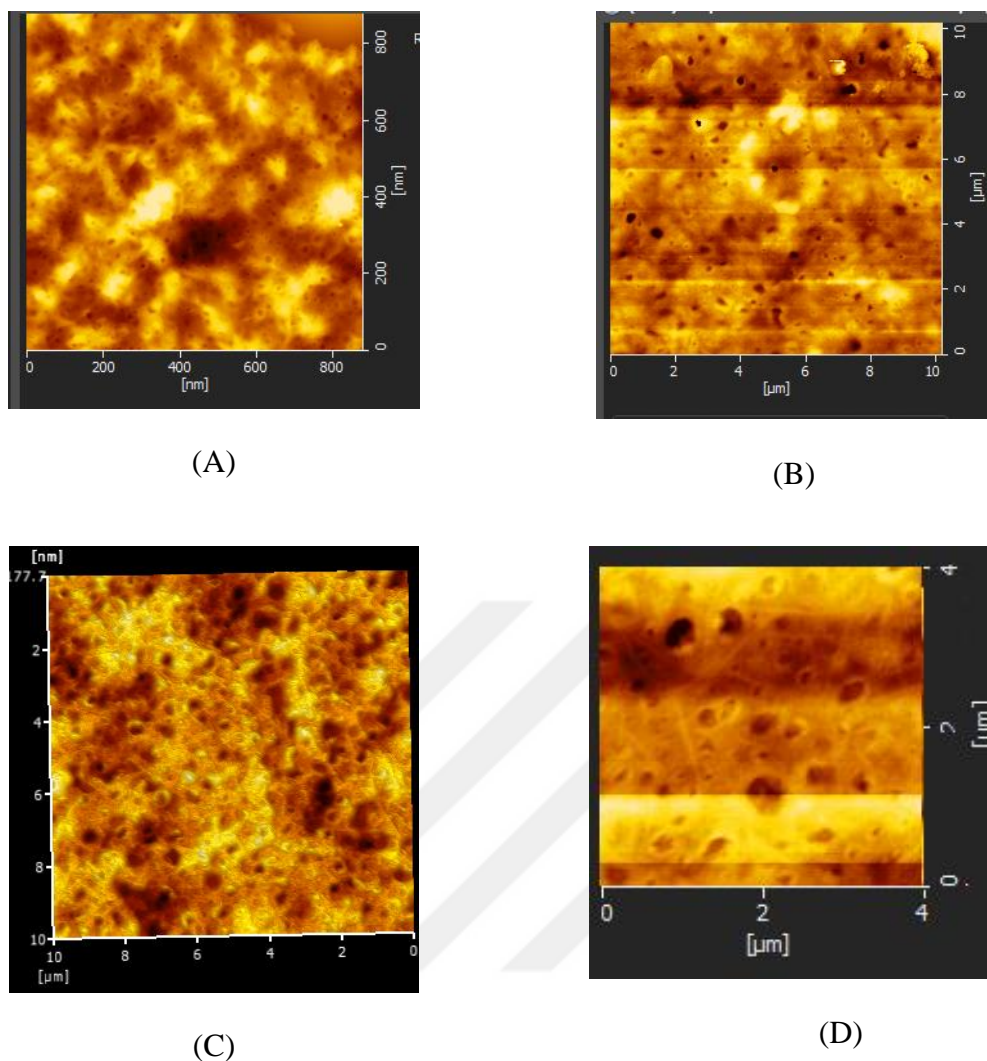


Figure 3.3. AFM topographic images and surface cross-section analysis of (A) blend 1 (1 $\mu\text{m} \times 1 \mu\text{m}$) (rms: 18.8 nm), (B) blend 2 (10 $\mu\text{m} \times 10 \mu\text{m}$) (rms: 21.7 nm), (C) blend 3 (10 $\mu\text{m} \times 10 \mu\text{m}$) (rms: 24.8 nm) and (D) blend 4 (4 $\mu\text{m} \times 4 \mu\text{m}$) (rms: 26 nm)

3.3 FT-IR

The strength of the hydrogen bond determines the extent of shifts in the IR-absorption frequencies of bonds formed between donor and acceptor sites in a molecule. This phenomenon might be interpreted as a proof of an energetic interaction between the blend components and, therefore their miscibility [104]. It is well known from previous studies that the FTIR spectrum of CH show peaks between 3500 cm^{-1} and 3100 cm^{-1} due to N-H and OH stretching bands and peaks at 1646 , 1588 and 1324 cm^{-1} correspond to the N-H bending, $-\text{NH}_2$ (amide II) and N-H bending(amide III), respectively. The C-O-C bending vibration of glucose rings and glycosidic linkages appeared at 1076 , 1021 , and 972 cm^{-1} respectively. For

pure PEO, the major absorption peaks appeared at 1098 and 843 cm^{-1} are due to the C-O-C symmetric bending vibration, and absorption bands at 1340 and 1359 cm^{-1} are due to the wagging vibrations of CH₂ groups in the crystalline phase [104,110]. In FTIR spectra of BC (Figure 3.4), a distinguish absorption peak at about 3340 cm^{-1} and a shouldering around 3240 cm^{-1} due to the O-H stretching. The peak at 1429 cm^{-1} is attributed to the symmetric bending of CH₂ and 1645 cm^{-1} is the glucose carbonyl of BC. The bands at 1162 cm^{-1} and 2894 cm^{-1} correspond to C-O-C asymmetric stretching and C-H stretching, respectively, and the peaks appeared at 1033 and 1056 cm^{-1} correspond to C=O stretching of BC [111, 112, 113].

The changes in the shape and intensity of the peaks at 1340 and 1359 cm^{-1} , which correspond to the CH₂ wagging vibration bands of crystalline PEO, indicate the interactions and hydrogen bonding between CH and PEO. These interactions also resulted in reduced crystallinity in PEO [104]. The 1344 cm^{-1} absorption band, which is associated with the CH₂ wagging vibration in the amorphous phase, is the result of merging these characteristic bands into a single absorption band. This phenomenon is attributed to the disruption of PEO morphological structure due to strong intermolecular interactions and the formation of hydrogen bonds between the -NH₂ groups of CH and etheric oxygen in PEO. Moreover, FT-IR results revealed that adding BC to the blend films resulted in an increased intermolecular interaction leading to a more amorphous morphological structure.

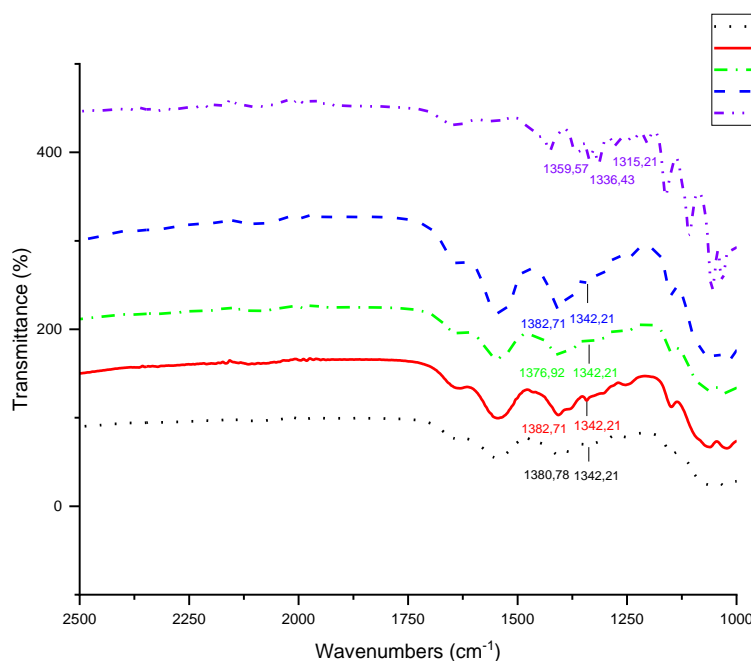


Figure 3.4. FTIR spectra of blends and BC

3.4 DSC

DSC is one of the most frequently used techniques among all thermal analysis methods since it is helpful for the investigation of the thermal behaviour of polymeric materials accompanied by heat absorption or release processes. The area under exothermic or endothermic peaks in a DSC thermogram and their corresponding peak temperature are characteristic and provide a quantitative measure for chemical and physical changes such as melting, crystallization, polymerization, glass transition, thermal decomposition etc. The heat absorbed during the melting process is a quantitative measure of the crystalline portion of the polymer mixture [106].

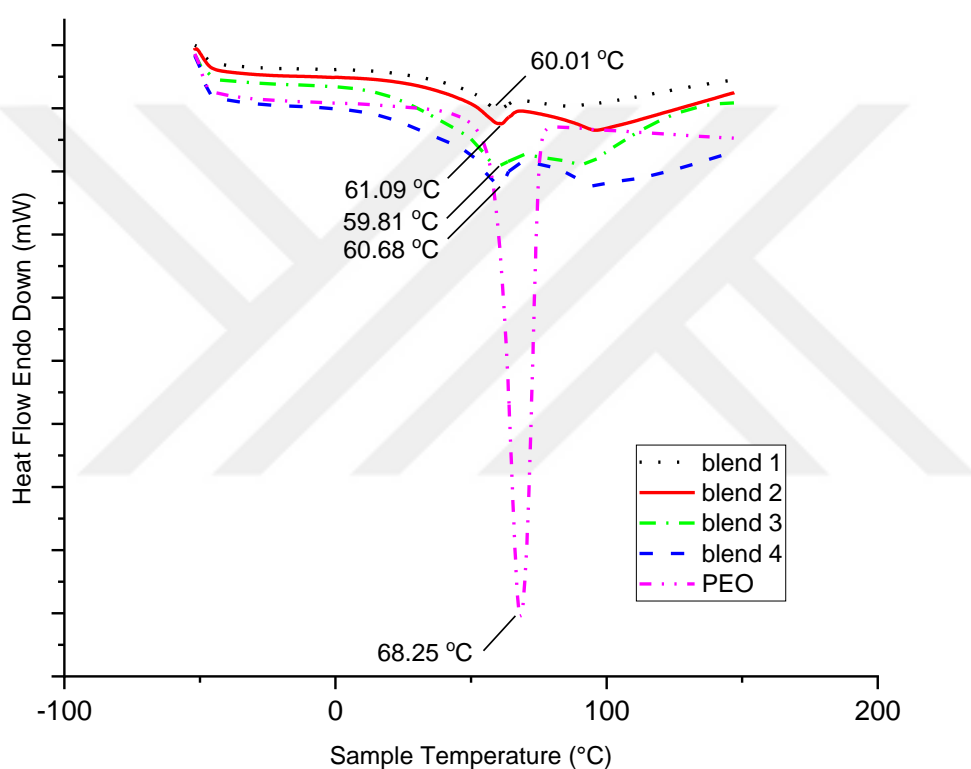
The morphological structure of blends and the effect of the increased amount of BC on blends were investigated using DSC. The comparative DSC thermograms of the blend films and pure PEO are shown in Figure 3.5 and the data obtained from DSC are collected in Table 3.2.

All thermograms show an endothermic peak at approximately 100 °C for all blends, which was attributed to the elimination of the surface water. This event is typical for cellulosic materials and CH due to the interaction of hydroxyl groups and water [104, 114].

Since BC and CH melting behaviors could not be observed in DSC thermograms, the calculated heat of fusion values from the melting peaks were attributed to PEO melting. While pure PEO displays a melting point at 68.25 °C, there is a noticeable decrease in the melting points of PEO in blends, which was at around 60.0 °C, indicating an energetic interaction taking place between C-O-C groups of PEO, and -NH₂ and -OH groups of CH. This interaction disrupted the PEO crystallization to some extent. Therefore, PEO in the blends showed relatively lower melting temperatures. On the other hand, the melting enthalpy of PEO in the blends increased with an increasing portion of BC, while the melting temperature remained nearly constant. Although the melting temperature of PEO did not change with increasing BC amount, the increase in melting enthalpy indicated that the BC interacted with PEO as well as CH chains. Bostan et al. reported that in PEO-CH blend systems, CH suppressed the PEO crystallinity up to 25 % of PEO portion of the blend systems. More amorphous blend structure was observed under this PEO percentage. The incorporation of PEO and CH into the porous structure of the BC increased the energetic interaction between the polymer chains, resulted in higher melting enthalpy of PEO.

Table 3.2. DSC data of the blends and pure PEO

Sample code	T_m (°C)	ΔH J/g
Blend 1	60.01062	3.9447
Blend 2	61.09236	5.8245
Blend 3	59.81144	8.8009
Blend 4	60.68555	10.5902
PEO	68.25	197

**Figure 3.5.** DSC curves of blends

3.5 TGA

Figure 3.6 shows TG curves of pure PEO and CH. These polymers display different thermal behavior. While PEO decomposition starts at 379 °C, CH decomposition starts at 318 °C. The thermal decomposition temperature of the PEO in the blend form is much higher than pure PEO (nearly 400 °C). This result was due to the intermolecular interaction between blend components.

The rate of weight loss and the thermal stability of the blend components separately are direct quantitative measure of the area under the DTG curves and their peak values. We could understand how an intermolecular interaction affects thermal stability of blends by comparing their DTG peak values [115].

The DTG curves of the blends (Figure 3.7) display three distinct peaks. The first peak between 64-100 °C is due to the water elimination from the blends. Second and third peak between 278-291 °C and 419-422 °C, respectively, corresponds maximum weight loss rate temperatures of CH and PEO, respectively. Moreover a neck shaped peak appeared around 200 °C which may attributed to the thermal degradation of the protein parts in blends. Similar studies in the literature also agree with these results [116, 104]. While the maximum weight loss temperature of pure PEO is 409 °C, the maximum weight loss temperature of PEO in blend 4 was 419.75 °C indicating an increased thermal stability of PEO in blends. However, when blends are compared to each other, there is a decrease in maximum weight loss temperatures with increasing amounts of BC, revealing an increased degradation rate, attributed to increased number of intermolecular interactions. These results are consistent with the intermolecular interactions confirmed by FTIR results. On the other hand, when the weight residues of blends are evaluated (Figure 3.8), it is seen that the weight residues of blends increase as the BC amount increases. These results can be concluded that adding BC in blend mixtures increased thermal stability and thermal degradation rates.

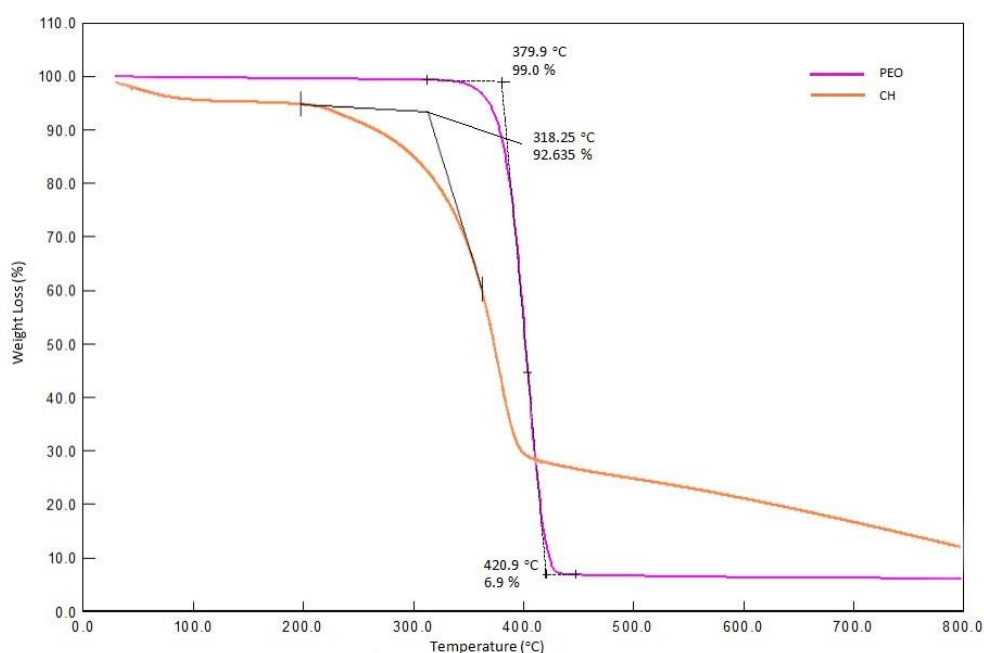


Figure 3.6.TG curves of CH and PEO

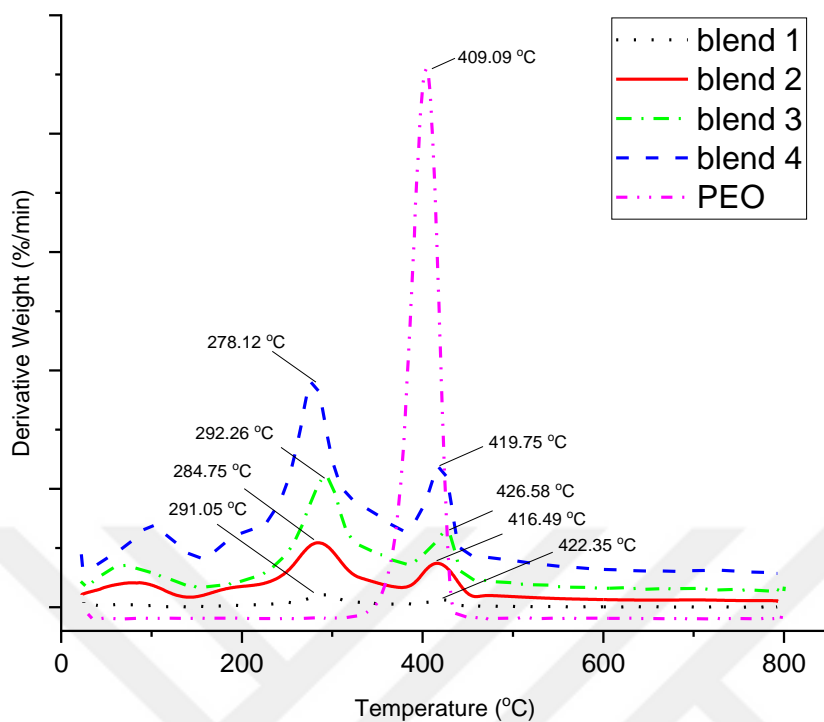


Figure 3.7.DTG curves of blends

Table 3.3. DTG peak temperature

Sample code	CH peak temperature (°C)	PEO Peak temperature (°C)
Blend 1	291.05	422.35
Blend 2	284.75	416.49
Blend 3	292.26	426.58
Blend 4	278.12	419.75
PEO	-	409.09

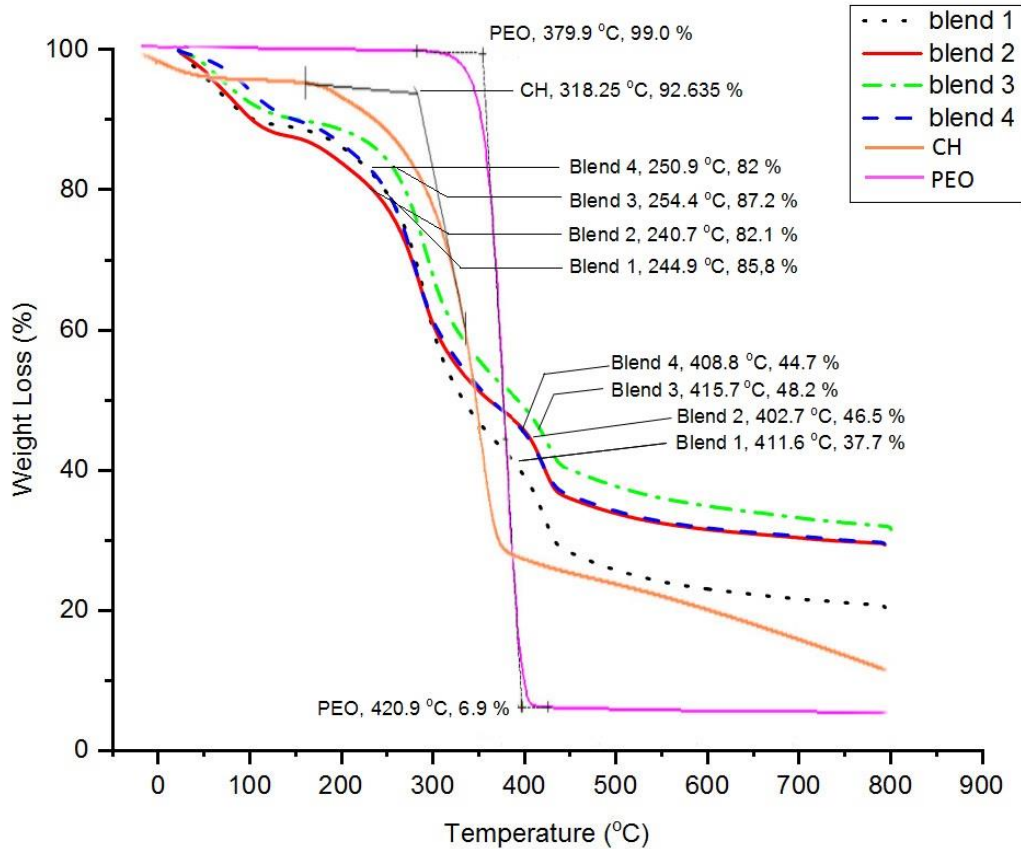


Figure 3.8. TG curves of the blends

3.6 Stress Strain

Stress-strain analysis of the blends was performed to determine the mechanical strength and the effect of increased amount of BC in PEO-CH formulations.

Stress resistance was measured for each sample. All samples were cut with a mold in dog-shape, and each measurement was repeated 3 times and averaged results were used.

The stress-strain curve indicated three zones during the deformation of the samples: elastic region (linear deformation stage), stable stage (plateau), and final stage, where the stress decreased rapidly.

PEO, a crystalline and hygroscopic polymer, has a low film capacity when used alone. Such attempts usually result in rigid, brittle films, making stress-strain testing difficult. It is also known from previous studies that PEO-CH inter molecular interactions and hydrogen bond formation increased the amorphous portions of PEO [104]. Addition of BC to CH-PEO blends slightly increases the mechanical properties of blends. In comparison to that of Blend 1, the tensile strength and elongation at break of Blend 4 increased with an increase of BC content.

The maximum tensile strength value was 3.95 Mpa and elongation at break was 11. %17 after adding % 6 (w/v) BC (Table 3.4).

Table 3.4. Mechanical properties

Sample code	Tensile strength (mPa)	Elongation at break (%)
Blend 1	2.86	9.99
Blend 2	3.11	10.21
Blend 3	3.56	10.53
Blend 4	3.95	11.17

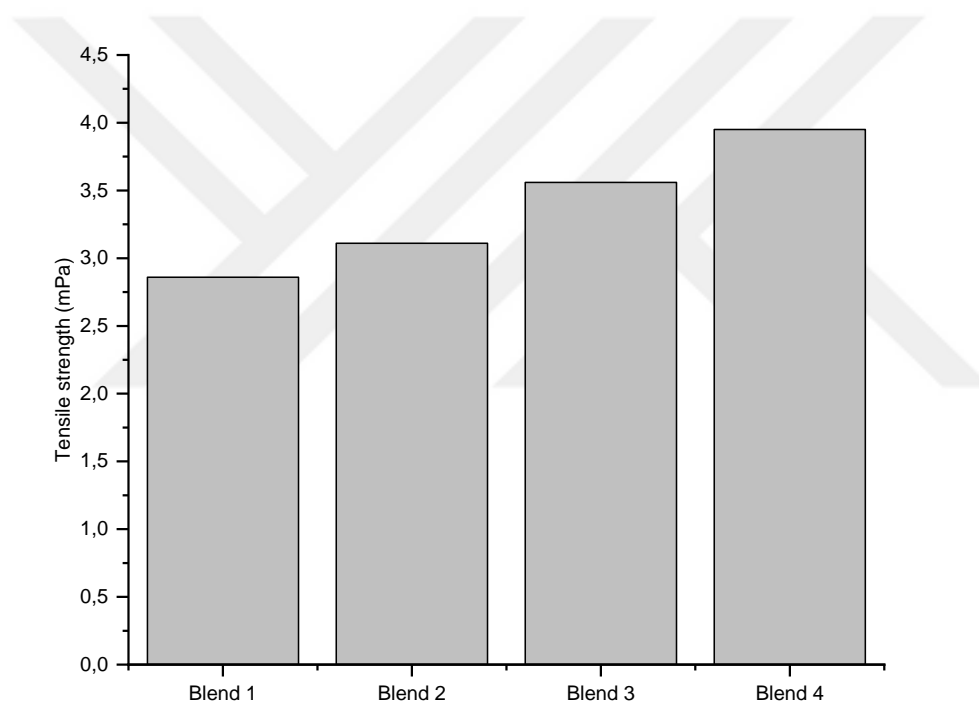


Figure 3.9.Tensile strength values of blends

3.7 DMA

The E' indicates the stiffness of the material. The temperature at which E' starts to decrease rapidly at any constant deformation rate is the T_g [108]. The $\tan \delta$ is a ratio that shows how much energy is lost as heat for every unit cycle of energy taken in and given back by the system. The T_g value can be obtained from the maximum peak position of the $\tan \delta$ curve as a

function of temperature. Moreover, it gives information about blend compatibility. The incompatible blends usually show two damping peaks indicating T_g 's of each polymeric component. Conversely, the compatible blend systems only display a single peak as a combined process. Figure 3.12 shows the $\tan \delta$ curves of blends as a function of temperature, and the observed single peaks are due to the single phase morphology indicating the compatibility of all blends. The T_g values of blends obtained from the maximum peak temperatures of $\tan \delta$ curves of blends are given in Table 3.5.

The increased shift in the T_g values and the increased value of E' conducted at 10 Hz (Figure 3.10) upon the addition of BC, may result from the restricted chain mobility of PEO due to the increased intermolecular interactions and hydrogen bonding. This improvement would be a high aspect ratio of BC capable of connecting between PEO and CH chains, which enhanced a large contact surface and, therefore, excellent coherence [116]. Furthermore, the porous structure of BC acts as filler, creating a node effect between PEO and CH chains, restricting the chain mobility, and increasing the values of T_g and E' values of blends. The decreasing trend in the E'' curve of blends as a function of time and temperatures is given in Figure 3.11, which is consistent with the E' curves.

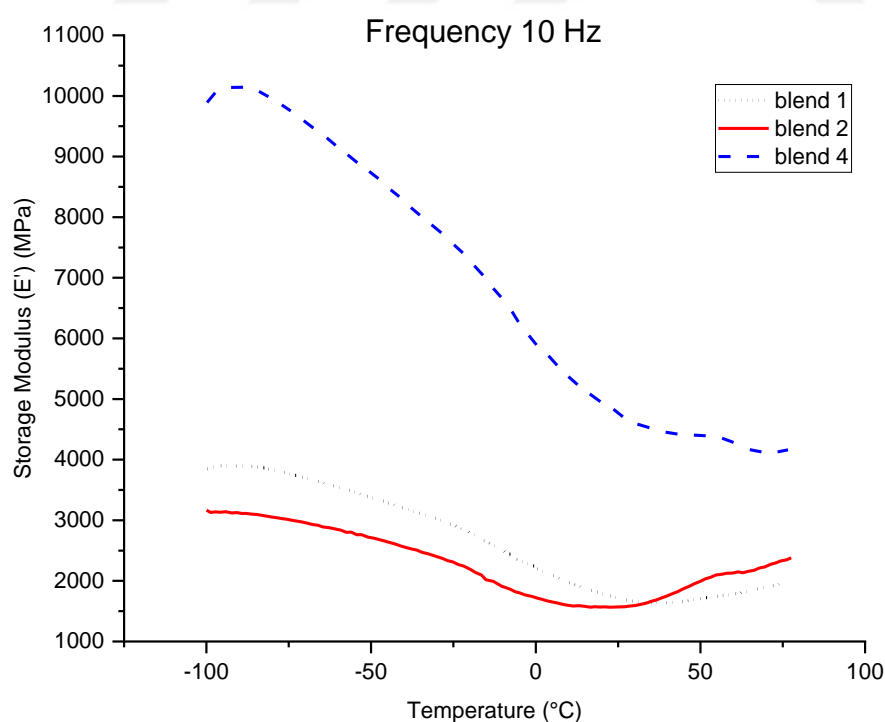


Figure 3.10. E' curves of blends

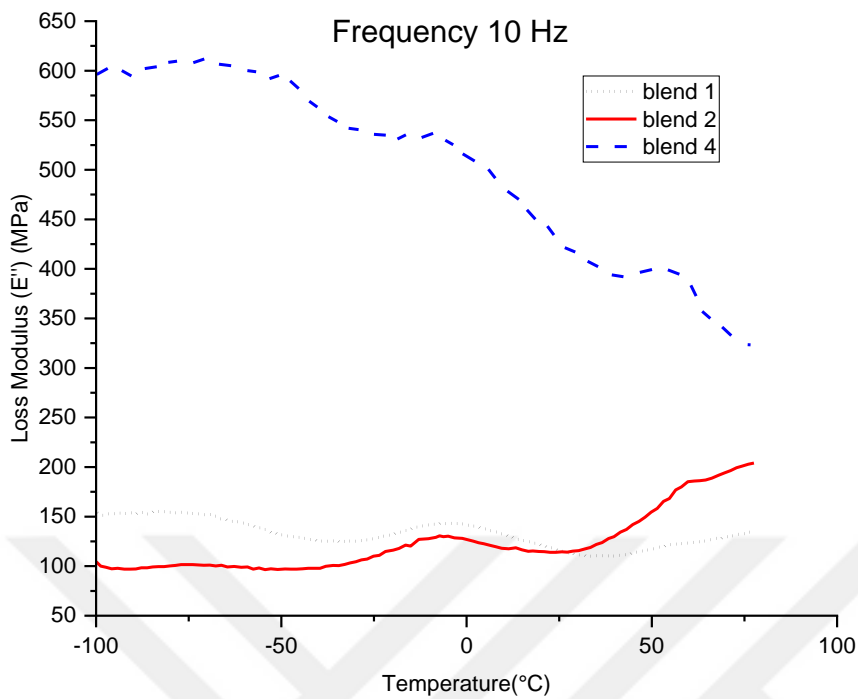


Figure 3.11. E'' curves of blends

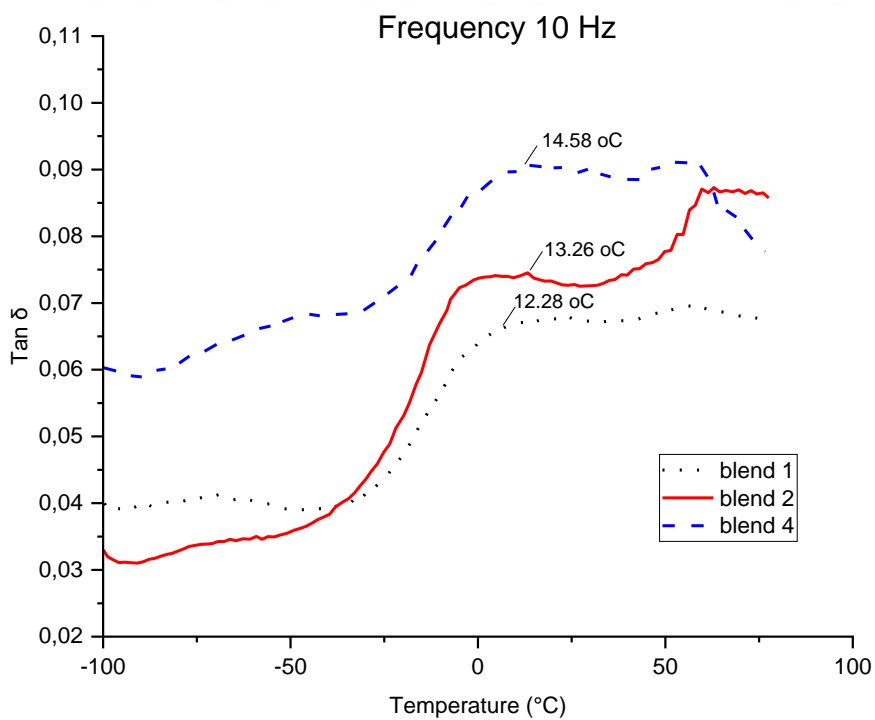


Figure 3.12. Tan δ curves of blends

Table 3.5. T_g values of blends

Sample code	T _g (°C)
Blend 1	12.28
Blend 2	13.26
Blend 4	14.58

Table 3.6. N values of blends

Sample code	N (moles/m ³)
Blend 1	230839.0762
Blend 2	190960.8236
Blend 3	239626.504
Blend 4	582583.7501

The storage modulus obtained from DMA also provides additional information about the entanglement of polymeric chains in blends. The entangled and compatible blends show a higher N than incompatible ones. The N value can be calculated by the equation 1 [108]:

$$N = \frac{E'}{6RT} \quad (\text{Equation 1})$$

Where E' denotes the storage modulus obtained from the E'-temperature curve, R denotes the universal gas constant, and T denotes the absolute temperature.

The calculated N values are given in Table 3.6. There is a significant increase in the N value of blend 4 compared to blend 1, which was attributed to increased entanglement of PEO and CH chains due to the filler effect of BC, leading to increased interaction time and formation of more vital intermolecular interaction. These results are also consistent with DSC results.

4 CONCLUSIONS

Conventional polymer-based packaging methods have harmful impacts on the environment and humans. An eco-friendly solution for reducing this problem has been desired for a long time. BC is the purest cellulose form that can be obtained from the microbes with the desired properties. Due to its biodegradability, biocompatibility and various other superior properties, BC is used as a packaging component for a while. However, BC alone is insufficient to maintain the appropriate packing qualities. Although BC has been used in different mixtures and forms in the past, it has never been found to be used with PEO and CH together. For this purpose, BC filled PEO-CH blends were desired to be prepared and characterized in light of the successful studies on binary PEO and CH blends, as well as the advantage of structural similarities of BC and CH. For this purpose, four distinct BC filled PEO-CH blends were formulated, evaluated, and compared to establish how the incorporation of BC affected the blends' thermal, mechanical, spectroscopic, morphological and surface properties. Blends were prepared based on a fixed ratio of CH-PEO (%85-%15) and different amounts of BC (%0, %2, %4, %6) filler. BC morphological structure was found to be crystalline and porous. The porous structure of BC particles provides many advantages and routes for increased interaction and hydrogen bond formation between PEO and CH chains. These interactions also further confirmed by FT-IR spectroscopy. Moreover, BC hindered the PEO crystallinity to some extent and this result was confirmed by FT-IR spectroscopy results.

BC's porous structure resulted in a relatively rough surface on the PEO-CH blend films which may be attributed to BC enrichment on the blend film surface.

Adding BC into the blend compositions increased the T_g value of PEO while conversely decreasing the melting point. This behavior was evaluated as a result of the increased intermolecular interaction of polymeric chains upon the addition of porous BC filler which prevents the segmental movements to some extent. The increased amount of BC in blend mixtures slightly increased the thermal stability and thermal degradation rates, and moreover both entanglement density and mechanical properties of blends increased as the BC was added to the blends. Based on these results, BC filled PEO-CH blends were successfully developed and showed a promising potential to be used in the food, pharmaceutical, and medical field.

REFERENCES

1. Barud, H.G.O., Silva, R.R., Barud, H.S., Tercjak, A., Gutierrez, J., Lustri, W.R., Junior, O.B.O, Ribeiro, S.J.L., (2016). A multipurpose natural and renewable polymer in medical applications: Bacterial cellulose, *Carbohydrate Polymers*, 153, 406-420.
2. Ullaha, H., Wahid, F., Santos, H.A., Khana, T. (2016). Advances in biomedical and pharmaceutical applications of functional bacterial cellulose-based nanocomposites. *Carbohydrate Polymers*, 150, 330-352.
3. Mohite, B.V., Patil, S.V. (2014). Physical, structural, mechanical and thermal characterization of bacterial cellulose by *G. hansenii* NCIM 2529. *106*, 132-141
4. Picheth, G.F., Pirich, C.L., Sierakowski, M.R., Woehl, M.A., Sakakibara, C.N., Souza, C.F., Martin, A.A., Silva, R., Freitas, R.A. (2017). Bacterial cellulose in biomedical applications: A review. *International Journal of Biological Macromolecules*, 104, 97-106.
5. Brown, R.M.J., Saxena, I.M. (2007). *Cellulose: Molecular and structural biology*, Springer, ISBN 978-1-4020-5332-0, New York, NY.
6. Jonas R, Farah LF. 1998. Production and application of microbial cellulose. *Polym Degrad Stabil*, 59, 101–106.
7. Watanabe K, Tabuchi M, Ishikawa A, Takemura H, Tsuchida T, Morinaga Y, Yoshinaga F. 1998. *Acetobacter xylinum* mutant with high cellulose productivity and an ordered structure. *Biosci Biotech Bioch*, 62(7), 1290– 1292.
8. El-Saied H, Basta AH, Gobran RH. 2004. Research progress in friendly environmental technology for the production of cellulose products (bacterial cellulose and its application). *Polym–Plast Technol*, 43(3), 797–820.
9. Johnson, D.C., Neogi, A.N. (1989). Sheeted products formed from reticulated microbial cellulose. US Patent, 4863565.
10. Reiniati, I., Hrymak, A.N., Margaritis, A. (2017). Recent developments in the production and applications of bacterial cellulose fibers and nanocrystals. *Critical Reviews in Biotechnology*, 37(4), 510-524.
11. Bielecki, S., Krystynowicz, A., Turkiewicz, M., Kalinowska, H. (2000). Bacterial Cellulose. In: Steinbuchel A (Ed), *Biopolymers: Polysaccharides I*, Wiley-VCH Verlag GmbH, 7, 37-90.

12. Ullah, H., Santos, H.A., Khan, T. (2016). Applications of bacterial cellulose in food, cosmetics and drug delivery. Springer, Cellulose, 23, 2291–231.
13. Islam, M., Khan, T., Park, J.K. (2012). Water holding and release properties of bacterial cellulose obtained by in situ and ex situ modification. Carbohydrate Polymers, 88(2), 596-603.
14. Chawla, P.R., Bajaj, I.B., Survase, S.A., Singhal, R.S. (2009). Microbial cellulose: fermentative production and applications. Food Technology Biotechnology, 47(2), 107-124.
15. Gayathry, G., Gopalswamy, G. (2014). Production and characterization of microbial cellulosic fibre from Acetobacter xylinum. Indian Journal of Fibre and Textile Research, 39, 93-96.
16. Treesuppharat, W., Rojanapanthu, P., Siangsano, C., Manuspiya, H., Ummartyotin, S. (2017). Synthesis and characterization of bacterial cellulose and gelatin-based hydrogel composites for drug-delivery systems. Biotechnology Reports, 15, 84-91.
17. Wang, J., Tavakoli, J., Tang, Y. (2019). Bacterial cellulose production, properties and applications with different culture methods – A review. Carbohydrate Polymers, 219, 63-76.
18. Esa F., Tasirin S.M., Rahman N.A. (2014). Overview of Bacterial Cellulose Production and Application. Agriculture and Agricultural Science Procedia 2, 113 – 119.
19. Shi Z., Zhang Y., Phillips G. O., Yang G. (2014). Utilization of bacterial cellulose in food. Food Hydrocolloids, 35, 539-545.
20. Chen P., Cho S.Y., Jin H.J., 'Modification and Applications of Bacterial Celluloses in Polymer Science', Macromolecular Research, Vol. 18, No. 4, 309-320, 2010.
21. Dayal, M.S., Catchmark, J.M. (2016). Mechanical and structural property analysis of bacterial cellulose composites. Carbohydrate Polymers, 144, 447-453.
22. Unal, S., Arslan, S., Yilmaz, B.K., Kazan, D., Oktar, F.,N., Gunduz, O. (2020). Glioblastoma cell adhesion properties through bacterial cellulose nanocrystals in polycaprolactone/gelatin electrospun nanofibers. Carbohydrate Polymers, 233, 115820.
23. Illa, M.P., Sharma, C.S., Khandelwal, M. (2019). Tuning the physiochemical properties of bacterial cellulose: effect of drying conditions. J Mater Sci, 54, 12024–12035.

24. Haghghi, H., Gullo, M., China, S., Pfeifer, F., Siesler, H.W., Licciardello, F., Pulvirenti, A. (2021). Characterization of bio-nanocomposite films based on gelatin/polyvinyl alcohol blend reinforced with bacterial cellulose nanowhiskers for food packaging applications. *Food Hydrocolloids*, 113, 106454.
25. Römling, U., Galperin, M.Y. (2015). Bacterial cellulose biosynthesis: diversity of operons, subunits, products, and functions. *Trends in Microbiology*, 23, 9, 545-557.
26. Picheth, G.F., Pirich, C.L., Sierakowski, M.R, Woehl, M.A., Sakakibara, C.N., Souza, C.F., Martin, A.A., Silva, R., Freitas, R.A. (2017). Bacterial cellulose in biomedical applications: A review. *International Journal of Biological Macromolecules*, 104 (A), 97-106.
27. Jonas, R., Farah, L.F. (1998). Production and application of microbial cellulose. *Polymer Degradation and Stability*, 59, 101-106.
28. Vandamme, E.J., De Baets, S., Vanbaelen, A., Joris, K., De Wulf P. (1998). Improved production of bacterial cellulose and its application potential. *Polymer Degradation and Stability*, 59(7), 93-99.
29. Ross, P., Mayer, R., Benziman, M. (1991). Cellulose biosynthesis and function in bacteria. *Microbiological Reviews*, 55(1), 35-58.
30. Cazóna, P., Vázquez, M. (2021). Bacterial cellulose as a biodegradable food packaging material: A review, 113, 106530.
31. Ramana, K., Tomar, A., Singh, L. (2000). Effect of various carbon and nitrogen sources on cellulose synthesis by *Acetobacter xylinum*. *World Journal of Microbiology and Biotechnology*, 16(3), 245-248.
32. Revin, V., Liyaskina, E., Nazarkina, M., Bogatyreva, A., Shchankin, M. (2018). Costeffective production of bacterial cellulose using acidic food industry by-products. *Brazilian Journal of Microbiology*, 49(1), 151-159.
33. Güzel, M., Akpınar, Ö. (2018). Production and characterization of bacterial cellulose from citrus peels. *Waste and Biomass Valorization*, DOI 10.1007/s12649-018-0241-x.
34. Carreira, P., Mendes, J.A., Trovatti, E., Serafim, L.S., Freire, C.S., Silvestre, A.J., Neto, C.P. (2011). Utilization of residues from agro-forest industries in the production of high value bacterial cellulose. *Bioresource Technology*, 102, 7354-7360.
35. Bae, S., Shoda, M. (2005). Production of bacterial cellulose by *Acetobacter xylinum* BPR2001 using molasses medium in a jar fermentor. *Applied Microbiology and Biotechnology*, 67, 45–51.

36. Hungund, B., Prabhu, S., Shetty, C., Acharya, S., Prabhu, V. (2013). Production of bacterial cellulose from *Gluconacetobacter persimmonis* GH-2 using dual and cheaper carbon sources. *Journal of Microbial and Biochemical Technology*, 5, 31-33.
37. Goelzer, F., Faria-Tischer, P., Vitorino, J., Sierakowski, M.R., Tischer, C. (2009). Production and characterization of nanospheres of bacterial cellulose from *Acetobacter xylinum* from processed rice bark. *Materials Science and Engineering*, 29, 546-551.
38. Chen, L., Hong, F., Yang, X.X. ve Han, S.F. (2012). Biotransformation of wheat straw to bacterial cellulose and its mechanism. *Bioresource Technology*, 135, 464-468.
39. Hong, F., Guo, X., Zhang, S., Han, S.F., Yang, G., Jönsson, L.J. (2012). Bacterial cellulose production from cotton-based waste textiles: enzymatic saccharification enhanced by ionic liquid pretreatment. *Bioresource Technology*, 104, 503- 508.
40. Usha, R.M., Appaiah, K.A. (2011). Statistical optimization of medium composition for bacterial cellulose production by *Gluconacetobacter hansenii* UAC09 using coffee cherry husk extract— an agro-industry waste. *Journal of Microbial and Biochemical Technology*, 21, 739-745.
41. Gomes, F.P., Silva, N.H., Trovatti, E., Serafim, L.S., Duarte, M.F., Silvestre, A.J., Neto, C.P., Freire C.S. (2013). Production of bacterial cellulose by *Gluconacetobacter sacchari* using dry olive mill residue. *Biomass Bioenergy*, 55, 205-211. 64.
42. Lin, D., Sanchez, P.L., Li, R., Li, Z. (2014). Production of bacterial cellulose by *Gluconacetobacter hansenii* CGMCC 3917 using only waste beer yeast as nutrient source. *Bioresource Technology*, 151, 113-119.
43. Mohammadkazemi, F., Azin, M., Ashori, A. (2015). Production of bacterial cellulose using different carbon sources and culture media. *Carbohydrate Polymers*, 117, 518-523.
44. Kızıldağ, E.E., Kızıldağ, A., Gardner, D.J. (2015). Synthesis of bacterial cellulose using hot water extracted wood sugars. *Carbohydrate Polymers*, 124, 131-138.
45. Cazóna, P., Velázquez, G., Vázquez, M. (2019). Characterization of bacterial cellulose films combined with chitosan and polyvinyl alcohol: Evaluation of mechanical and barrier properties. *Carbohydrate Polymers*, 216, 72-85.
46. Ul Islam, M., Ullah, M.W., Khan, S., Shah, N., Park, J.K. (2017). Strategies for cost-effective and enhanced production of bacterial cellulose. *International Journal of Biological Macromolecules*, 102, 116-1173.

47. 47. Watanabe K, Tabuchi M, Morinaga Y, Yoshinaga F. 1998a. Structural features and properties of bacterial cellulose produced in agitated culture. *Cellulose*, 5, 187–200.
48. Shah, N., Ul-Islam, M., Khattak, W. A., Park, J. K. (2013). Overview of bacterial cellulose composites: A multipurpose advanced material. *Carbohydrate Polymers*, 98, 1585– 1598.
49. 49. Bielecki, S., Krystynowicz, A., Turkiewicz, M., Kalinowska, H. (2000). Bacterial Cellulose. In: Steinbuechel A (Ed), *Biopolymers: Polysaccharides I*. Wiley-VCH Verlag GmbH, 7, 37-90.
50. Krystynowicz, A., Turkiewicz, M., Drynska, E., Galas, E. (1995). Bacterial cellulose biosynthesis and application. *Biotechnologia*, 30, 120-132.
51. Krystynowicz, A., Czaja, W., Pomorski, L., Kolodziejczyk, M., Bielecki, S. (2000). The evaluation of usefulness of microbial cellulose as a wound dressing material. 14th Forum for Applied Biotechnology, 27 28 September 2000, Gent, Belgium.
52. Yamanaka, S., Watanabe, K., Suzuki, Y. (1990). Hollow microbial cellulose, process for preparation thereof, and artificial blood vessel formed of said cellulose. European patent 0396344A2.
53. Klemm, D., Schumann, U., Udhardt, U., Marsch, S. (2001). Bacterial synthesized cellulose – artificial blood vessels for microsurgery. *Progress in Polymer Science*, 26(9), 1561-1599.
54. Kirdponpattara, S., Phisalaphong, M., Kongruang, S. (2017). Gelatin-bacterial cellulose composite sponges thermally cross-linked with glucose for tissue engineering applications. *Carbohydrate Polymers*, 177, 361-368.
55. Yan, H., Huang, D., Chen, X., Liu, H., Feng, Y., Zhao, Z., Dai, Z., Zhang, X., Lin, Q. (2018). A novel and homogeneous scaffold material: preparation and evaluation of alginate/bacterial cellulose nanocrystals/collagen composite hydrogel for tissue engineering. *Polymer Bulletin*, 75, 9185-1000.
56. Piasecka-Zelga, J., Zelga, P., Szulc, J., Wietecha, J., Ciechańska, D. (2018). An in vivo biocompatibility study of surgical meshes made from bacterial cellulose modified with chitosan. *International Journal of Biological Macromolecules*, 116, 1119-1127.
57. Yang, Q., Ma, H., Dai, Z., Wang, J., Dong, S., Shen, J., Dong, J. (2017). Improved thermal and mechanical properties of bacterial cellulose with the introduction of collagen. *Springer, Cellulose*, 24, 3777, 3787.

58. Çakmak, A.M., Unal, S., Sahin, A., Oktar, F.N., Sengor, M., Ekren, N., Gunduz, O., Kalaskar, D.M. (2020). 3D Printed Polycaprolactone/Gelatin/Bacterial Cellulose/Hydroxyapatite Composite Scaffold for Bone Tissue Engineering. *Polymers*, 12, 1962.
59. Luo, H., Xiong, G., Li, Q., Ma, C., Zhu, Y., Guo, R., Wan, Y. (2014). Preparation and Properties of a Novel Porous Poly(lactic acid) Composite Reinforced with Bacterial Cellulose Nanowhiskers. *Fibers and Polymers*, 15 (12), 2591-2596.
60. Maver, T., Kurecic, M., Pivec, T., Maver, U., Gradisnik, L., Gasparic, P., Kaker, B., Bratusa, A., Hribernik, S., Kleinschek, K.S.(2020). Needleless electrospun carboxymethyl cellulose/polyethylene oxide mats with medicinal plant extracts for advanced wound care applications. Springer, Cellulose.
61. Gallegos, A.V.A., Carrera, S.H., Parra, R., Keshavarz, T., Iqbal, M.N. (2016). Bacterial Cellulose: A Sustainable Source to Develop Value-Added Products – A Review. *BioResources*, 11(2), 5641-5655.
62. Pacheco, G., Mello, C.V., Chiari-Andreo, B.G., Isaac, V.L.B., Jose, S., Ribeiro, L., Pecoraro, E., Trovatti, E. (2018). Bacterial cellulose skin masks—Properties and sensory tests. *Journal of Cosmetic Dermatology*, 17, 840–847.
63. Numata, Y., Kono, H., Tsuji, M., Tajima, K. (2017). Structural and mechanical characterization of bacterialcellulose–polyethylene glycol diacrylate composite gels. *Carbohydrate Polymers*, 173, 67-76.
64. Shi, Z., Zhang, Y., Phillips, G.O., Yang, G. (2014) Utilization of bacterial cellulose in food. *Food Hydrocolloids*, 35, 539-545.
65. Ng, C., Sheu, F., Wang, C., Shyu, Y. (2004). Fermentation of *Monascus purpureus* on agri-byproducts to make colorful and functional bacterial cellulose (NATA). *Microbiology Indonesia*, 4(1), 6- 10.
66. 64. Ng, C., Shyu, Y.T. (2004). Development and production of cholesterol-lowering *Monascus-nata* complex. *World Journal of Microbiology and Biotechnology*, 20, 875-879.
67. 65. Stephens, S.R., Westland, J.A., Neogi, A.N. (1990). Method of using bacterial cellulose as a dietary fiber component. US patent 4960763.
68. 66. Lin, K.W., Lin, H.Y. (2004). Quality characteristics of Chinese-style meatball containing bacterial cellulose (Nata). *Journal of Food Science*, 69(3), 107-111.

69. 67. Lin, S.B., Chen, L.C., Chen, H.H. (2011). Physical characteristics of surimi and bacterial cellulose composite gel. *Journal of Food Process Engineering*, 34, 1363-1379.
70. 68. Çakmakçı, M.L., Karahan, A.G., Çakır, İ., Gündoğdu, A., Akoğlu, A. (2008). Selüloz üretiminde kullanılacak mikroorganizmaların izolasyonu, moleküler tanısı ve mikrobiyel selülozun gıda sanayinde kullanım olanaklarının araştırılması. TÜBİTAK, TOVAG 105O156.
71. Okiyama, A., Motoki, M., Yamanaka, S. (1992). Bacterial cellulose II. Processing of the gelatinous cellulose for food materials. *Food Hydrocolloids*, 6(5), 479-487.
72. Okiyama, A., Motoki, M., Yamanaka, S. (1993). Bacterial cellulose IV. Application to processed foods. *Food Hydrocolloids*, 6(6), 503-511.
73. Iguchi, M., Mitsuhashi, S., Ichimura, K. (1988). Bacterial cellulose-containing molding material having high dynamic strength. US Patent 4,742,164.
74. Krystynowicz, A., Czaja, W., Bielecki, S. (1999). Biosynthesis and application of bacterial cellulose. *Zywnosc*, 3, 22-33.
75. Johnson, D.C., Neogi, A.N. (1989). Sheeted products formed from reticulated microbial cellulose. US Patent, 4863565.
76. Wen, Y., Liu, J., Jiang, L., Zhu, Z., He, S., He, S., Shao, W. (2021). Development of intelligent/active food packaging film based on TEMPO-oxidized bacterial cellulose containing thymol and anthocyanin-rich purple potato extract for shelf life extension of shrimp. *Food Packaging and Shelf Life*, 29, 100709.
77. Fabra, M.J., Lopez-Rubio, A., Ambrosio-Martin, J., Lagaron, J.M. (2016). Improving the barrier properties of thermoplastic corn starch-based films containing bacterial cellulose nanowhiskers by means of PHA electrospun coatings of interest in food packaging. *Food Hydrocolloids*, 61, 261-268.
78. Xu, Y., Liu, X., Jiang, Q., Yu, D., Xu, Y., Wang, B., Xia, W. (2021). Development and properties of bacterial cellulose, curcumin, and chitosan composite biodegradable films for active packaging materials. *Carbohydrate Polymers*, 260, 117778.
79. Juntaroa, J., Ummartyotin, S., Saina, M., Manuspiya, H. (2012). Bacterial cellulose reinforced polyurethane-based resin nanocomposite: A study of how ethanol and processing pressure affect physical, mechanical and dielectric properties. *Carbohydrate Polymers*, 87, 2464-2469.

80. Gao, C., Yan, T., Du, J., He, F., Luo, H., Wan, Y. (2014). Introduction of broad spectrum antibacterial properties to bacterial cellulose nanofibers via immobilising ϵ -polylysine nanocoatings. *Food Hydrocolloids*, 36, 204-211.
81. Tome, L.C., Brandão, L., Mendes, A.M., Silvestre, A.J., Neto, C.P., Gandini, A. (2010). Preparation and characterization of bacterial cellulose membranes with tailored surface and barrier properties. *Cellulose*, 17(6), 1203-1211.
82. Xiao, L., Mai, Y., He, F., Yu, L., Zhang, L., Tang, H. (2012). Bio-based green composites with high performance from poly (lactic acid) and surfacemodified microcrystalline cellulose. *Journal of Materials Chemistry*, 22(31), 15732-15739.
83. Jayakumar, R., Prabakaran, M., Muzzarelli, R.A.A. (2011). Chitosan for Biomaterials II. *Advances in Polymer Science*, 244.
84. Azmana, M., Mahmood, S., Hilles, A.R., Rahman, A., Bin Arifin, M.A., Ahmed, S. (2021). A review on chitosan and chitosan-based bionanocomposites: Promising material for combatting global issues and its applications. *International Journal of Biological Macromolecules*, 185, 832-848.
85. Islam, S., Rahman Bhuiyan, M.A., Islam, M.N. (2017). Chitin and Chitosan: Structure, Properties and Applications in Biomedical Engineering. *Journal of Polymers and Environment*, 25, 854-866.
86. Meng, Q., Sun, Y., Cong, H., Hu, H., Xu, F. (2021). An overview of chitosan and its application in infectious diseases. *Drug Delivery and Translational Research*, 11, 1340-1351.
87. Kalia, S., Sabaa, M. W. (2013). *Polysaccharide Based Graft Copolymers*. Springer-Verlag Berlin Heidelberg.
88. Gautam, S., Chou, C., Dinda, A.K., Potdar, P.D., Mishra, N.C. (2014). Fabrication and characterization of PCL/gelatin/chitosan ternary nanofibrous composite scaffold for tissue engineering applications. *Journal of Materials Science*, 49, 1076-1089.
89. Bianchet, R.T., Cubas, A.L.V., Machado, M.M., Moecke, E.H.S. (2020). Applicability of bacterial cellulose in cosmetics – bibliometric review. *Biotechnology Reports*, 27, e00502.
90. Gularte, M.S., Anghinoni, J.M., Abenante, L., Voss, G.T., Oliveirac, R.L., Vaucher, R.A., Luchese, C., Wilhelmc, E.A., Lenardao, E.J., Fajardoa, A.R. (2019). Synthesis of chitosan derivatives with organoselenium and organosulfur compounds:

- Characterization, antimicrobial properties and application as biomaterials. *Carbohydrate Polymers*, 219, 240-250.
91. Kiuchi, H., Kai, W., Inoue, Y. (2008). Preparation and Characterization of Poly(ethylene glycol) Crosslinked Chitosan Films. *Journal of Applied Polymer Science*, 107, 3823-3830.
92. Afonso, C.R., Hirano, R.S., Gaspar, A.L., Chagas, E.G.L., Carvalho, R.A., Silva, F.V., Leonardi, G.R., Lopes, P.S., Silva, C.F., Yoshida, C.M.P. (2019). Biodegradable antioxidant chitosan films useful as an anti-aging skin mask. *International Journal of Biological Macromolecules*, 132, 1262-1273.
93. Ionescu, O.M., Iacob, A.T., Mignon, A., Vlierberghe, S.V., Baican, M., Danu, M., Ibanescu, C., Simionescu, N., Profire, L. (2021). Design, preparation and in vitro characterization of biomimetic and bioactive chitosan/polyethylene oxide based nanofibers as wound dressings. *International Journal of Biological Macromolecules*, 193, 996-1008.
94. Pathalamuthu, P., Siddharthan, A., Giridev, V.R., Victoria, V., Thangam, R., Sivasubramanian, S., Savariar, V., Hemamalini, T. (2019). Enhanced performance of Aloe vera incorporated chitosan-polyethylene oxide electrospun wound scaffold produced using novel Spirograph based collector assembly. *International Journal of Biological Macromolecules*, 140, 808-824.
95. Obeid, K.A.A., Al-Bermany, A.K.J., Habeeb, M.A. (2015). Enhancement of Some Mechanical Properties of Polyethylene Glycol by Adding Carboxymethyl Cellulose as a Blends and Applied in Wood Glue. *World Scientific News*, 21, 12-23.
96. Majdanski, T.B., Vitz, J.V., Meier, A., Brunzel, M., Schubert, S., Nischang, I., Schubert, U.S. (2018). "Green" ethers as solvent alternatives for anionic ring-opening polymerizations of ethylene oxide (EO): In-situ kinetic and advanced characterization studies. *Polymer*, 159, 86-94.
97. Zivanovic S., Li J., Davidson P.M., Kit K. (2007). Physical, Mechanical, and Antibacterial Properties of Chitosan/PEO Blend Films. *Biomacromolecules*, 8, 1505-1510.
98. Morsi, M.A., Abdelaziz, M., Oraby, A.H., Mokhles, I. (2018). Effect of lithium titanate nanoparticles on the structural, optical, thermal and electrical properties of polyethylene oxide/ carboxymethyl cellulose blend. *Journal of Materials Science: Materials in Electronics*, 29, 15912–15925.

99. Morsia, M. A., Abdelaziz, M., Oraby, A.H., Mokhles, I. (2019). Structural, optical, thermal, and dielectric properties of polyethylene oxide/ carboxymethyl cellulose blend filled with barium titanate. *Journal of Physics and Chemistry of Solids*, 125, 103-114.
100. Draksler, P., Jankovic, B., Abramovic, Z., Lavric, Z., Meden, A. (2019). Assessment of critical material attributes of polyethylene oxide for formulation of prolonged release tablets. *Drug Development And Industrial Pharmacy*, 45:12, 1949-1958.
101. Menazea, A. A. (2020). Pulsed laser ablation route assisted copper oxide nanoparticles doped in Polyethylene Oxide/Polyvinyl pyrrolidone blend for enhancement the electrical conductivity. *Journal of Molecular Structure*, 1207, 127807.
102. Rajeha, A., Morsi, M. A., Elashmawi, I.S. (2019). Enhancement of spectroscopic, thermal, electrical and morphological properties of polyethylene oxide/carboxymethyl cellulose blends: Combined FT-IR/DFT. *Vacuum*, 159, 430-440.
103. Aki, D., Ulag, S., Unal, S., Sengor, M., Ekren, N., Lin, C.C., Yilmazer, H., Ustundag, C.B., Kalaskar, D.M., Gunduz, O. (2020). 3D printing of PVA/hexagonal boron nitride/bacterial cellulose composite scaffolds for bone tissue engineering. *Materials and Design*, 196, 109094.
104. Bostan, M. S., Mutlu, A. C., Kazak, H., Keskin., S.S., Oner, E.T., Eroglu, M.S. (2014). Comprehensive characterization of chitosan/PEO/levan ternary blend films. *Carbohydrate Polymers*, 102, 993-1000.
105. Joshi, J., Homburg, S.V., Ehrmann, A. (2022). Atomic Force Microscopy (AFM) on Biopolymers and Hydrogels for Biotechnological Applications—Possibilities and Limits. *Polymers*, 14, 1267.
106. Haines, P.J., Laye, P.G. (2002). *Principles of Thermal Analysis and Calorimetry*. The Royal Society of Chemistry.
107. Kumar, M.S.C., Alagar, M., Prabu, A.A. (2003). Studies on dynamic mechanical and mechanical properties of vinyloxyaminosilane grafted ethylene propylene diene terpolymer/linear low density polyethylene (EPDM-g-VOS/LLDPE) blends. *European Polymer Journal*, 39, 805-816.
108. Komalan, C., George, K.E., Kumar, P.A.S., Varughese, K.T., Thomas, S. (2007). Dynamic mechanical analysis of binary and ternary polymer blends based on nylon

- copolymer/EPDM rubber and EPM grafted maleic anhydride compatibilizer. *Express Polymer Letters*, 1:10, 641–653.
109. Beekmans, L. G. M., Van Der Meer, D. W., Vancso, G. J. (2002). Crystal melting and its kinetics on poly (ethylene oxide) by in situ atomic force microscopy. *Polymer*, 43, 1887-1895.
110. Pucić, I., Jurkin, T. (2012). FTIR assessment of poly(ethylene oxide) irradiated in solid state, melt and aqueous solution. *Radiation Physics and Chemistry*, 81:9, 1426-1429.
111. Jia, R., Wang, X., Huo, M., Zhai, X., Li, F., Zhong, C. (2017). Preparation and characterization of a novel bacterial cellulose/chitosan bio-hydrogel. *Nanomaterials and Nanotechnology*, 7,1-8.
112. Ye, J., Guo, L., Zheng, S., Feng, Y., Zhang, T., Yang, Z., Yuan, Q., Shen, G., Zhang, Z. (2019). Synthesis of bacterial cellulose based SnO₂-PPy nanocomposites as potential flexible, highly conductive material. *Materials Letters*, 253, 372-376.
113. Yanti, N. A., Ahmad, S. W., Muhiddin, N. H., Ramadhan, A. N., Walhidayah, S., Walhidayah, T. (2021). Characterization of Bacterial Cellulose Produced by *Acetobacter xylinum* Strain LKN6 Using Sago Liquid Waste as Nutrient Source. *Pakistan Journal of Biological Sciences*, 24, 335-344.
114. Oliveira, R. L., Vieira, J. G., Barud, H. S., Assunção, R. M. N., Filho, G. R., Ribeiro, S. J. L., Messadeqqa, Y. (2015). Synthesis and Characterization of Methylcellulose Produced from Bacterial Cellulose under Heterogeneous Condition. *J. Braz. Chem. Soc.*, 26, 9, 1861-1870.
115. Potivara, K., Phisalaphong, M. (2019). Development and Characterization of Bacterial Cellulose Reinforced with Natural Rubber. *Materials*, 12:14, 2323.
116. Sukyai, P., Sriroth, K., Lee, B. H., Kim, H. J. (2012). The effect of bacterial cellulose on the mechanical and thermal expansion properties of kenaf/poly(lactic acid) composites. *Applied Mechanics and Materials*. 117, 119, 1343-1351.

APPENDIXES

Appendix A

Weight losses of blends

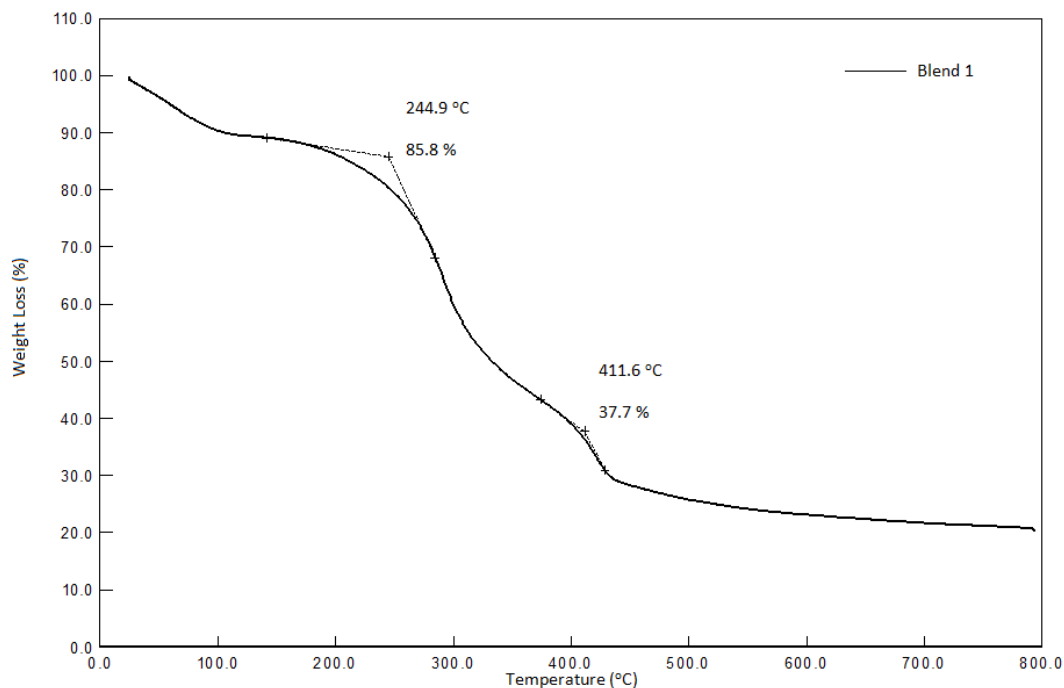


Figure A.1. Weight loss of blend 1

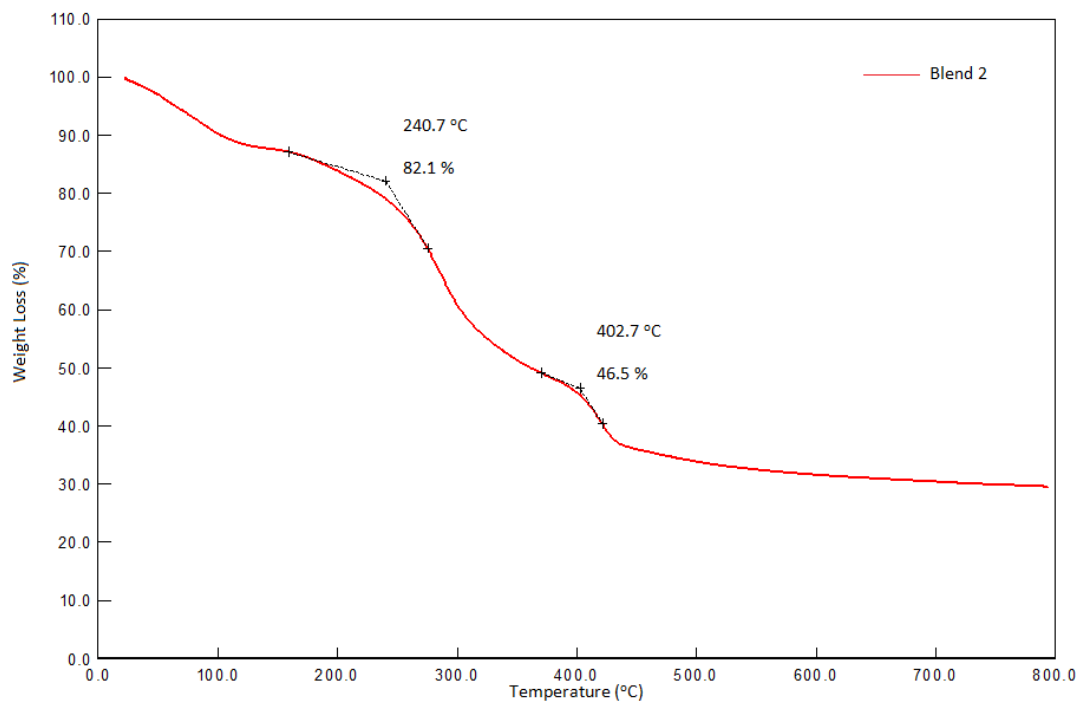


Figure A.2. Weight loss of blend 2

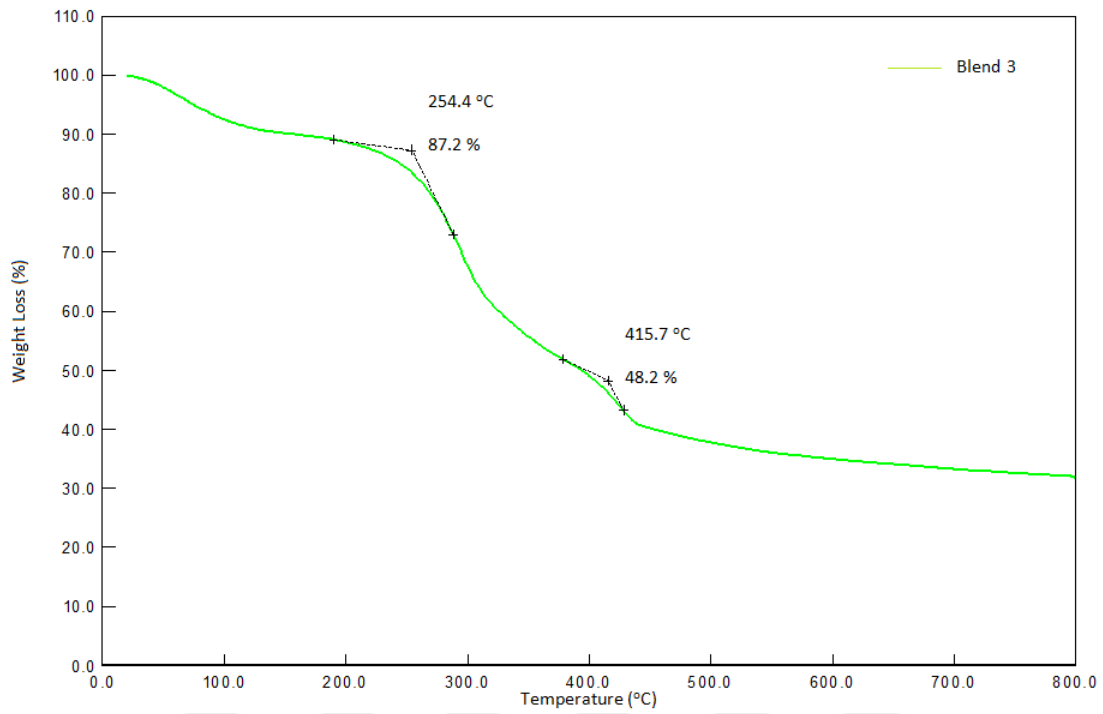


Figure A.3. Weight loss of blend 3

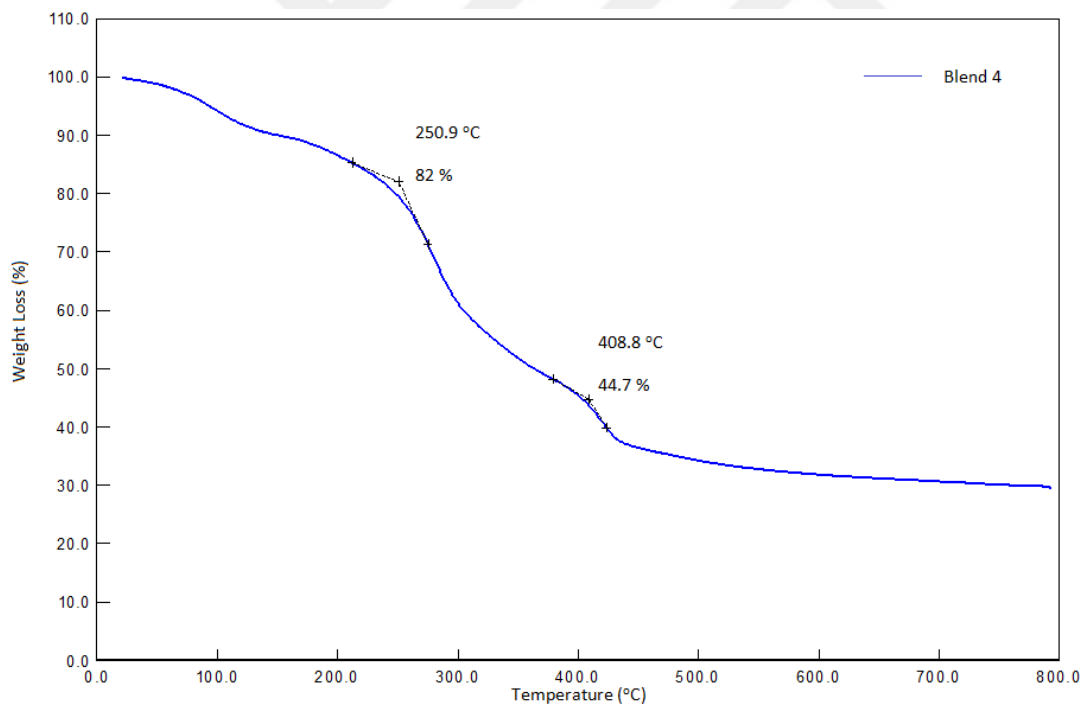


Figure A.4. Weight loss of blend 4

Appendix B

Weight losses of PEO and CH

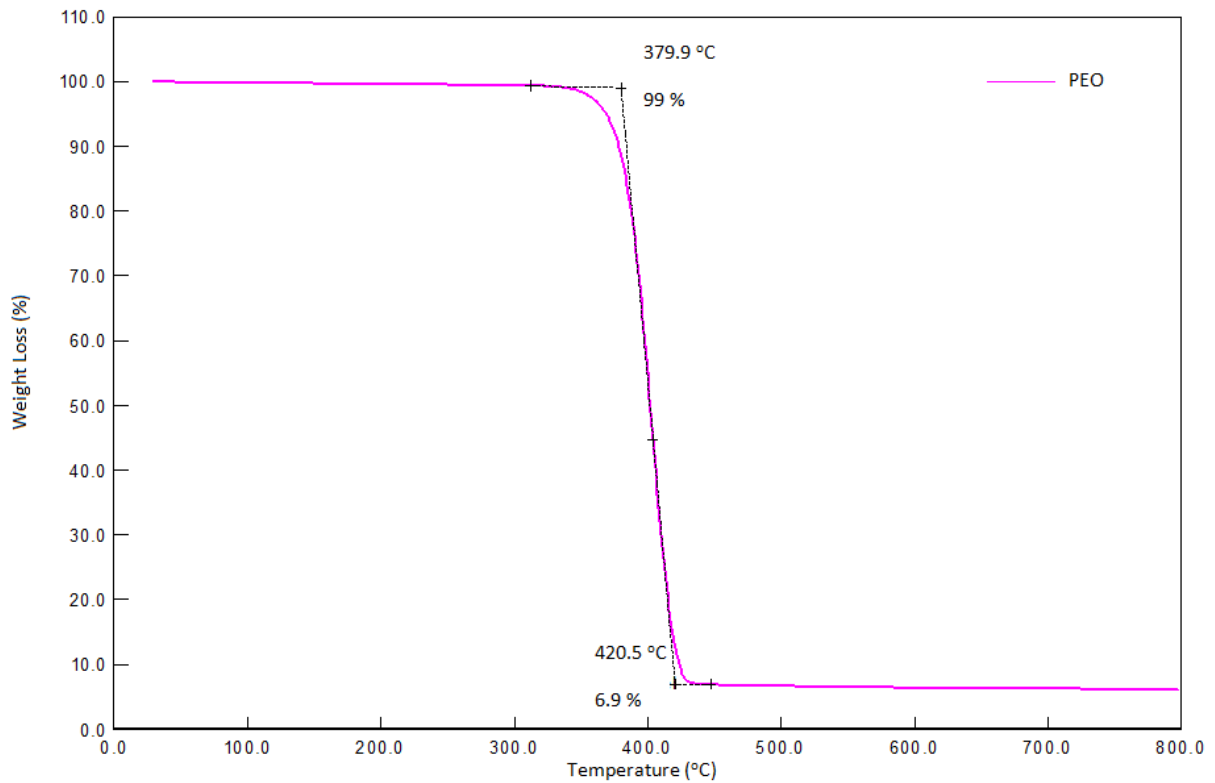


Figure B.1. Weight loss of PEO

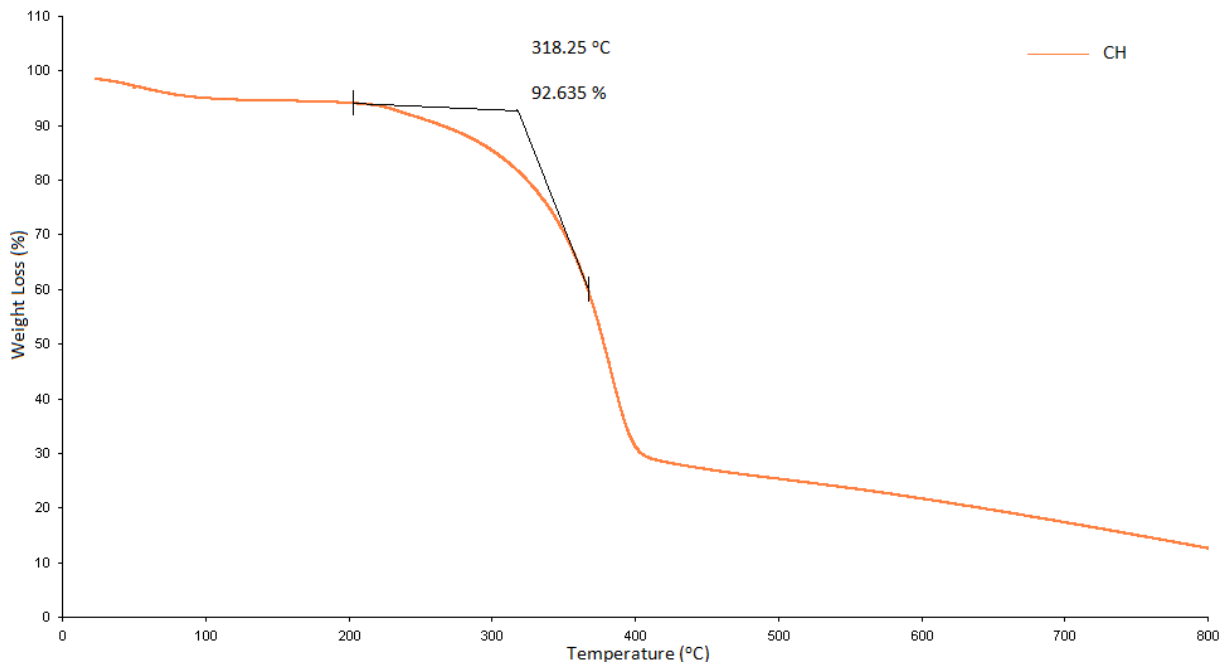


Figure B.2. Weight loss of CH

AUTOBIOGRAPHY

Name Surname : Fatmanur Ilhan

Language : English

Education

Degree	Department/Program	University/High School	Graduation Year
High school	Science	Nakipoğlu Cumhuriyet Anatolian High School	2011
Bachelor of Science	Chemical Engineering	Ege University	2016

Congress/Conference

Fatmanur Sarıgül, Müge Sennaroğlu Bostan, Mehmet Sayıp Eroğlu. "Preparation and Characterization of Bacterial Cellulose and Polyethylene Oxide Blend Films", International Natural Science, Engineering and Material Technologies Conference, Istanbul, Turkey.